NeuroImage 98 (2014) 243–257

Contents lists available at ScienceDirect

NeuroImage

journal homepage: www.elsevier.com/locate/ynimg

Human cortical areas involved in perception of surface glossiness

Atsushi Wada *, Yuichi Sakano, Hiroshi Ando

[a] Universal Communication Research Institute, National Institute of Information and Communications Technology, 3-5 Hikaridai, Seikacho, Sorakugun, Kyoto 619-0289, Japan
[b] Center for Information and Neural Networks (CiNet), National Institute of Information and Communications Technology and Osaka University, 1-4 Yamadaoka, Suita, Osaka 565-0871, Japan

ARTICLE INFO

Article history:
Accepted 4 May 2014
Available online 11 May 2014

Keywords:
Specular reflection
Surface property
Feature-based attention
fMRI
Material perception

ABSTRACT

Glossiness is the visual appearance of an object's surface as defined by its surface reflectance properties. Despite its ecological importance, little is known about the neural substrates underlying its perception. In this study, we performed the first human neuroimaging experiments that directly investigated where the processing of glossiness resides in the visual cortex. First, we investigated the cortical regions that were more activated by observing high glossiness compared with low glossiness, where the effects of simple luminance and luminance contrast were dissociated by controlling the illumination conditions (Experiment 1). As cortical regions that may be related to the processing of glossiness, V2, V3, hV4, VO-1, VO-2, collateral sulcus (CoS), LO-1, and V3A/B were identified, which also showed significant correlation with the perceived level of glossiness. This result is consistent with the recent monkey studies that identified selective neural response to glossiness in the ventral visual pathway, except for V3A/B in the dorsal visual pathway, whose involvement in the processing of glossiness could be specific to the human visual system. Second, we investigated the cortical regions that were modulated by selective attention to glossiness (Experiment 2). The visual areas that showed higher activation to attention to glossiness than that to either form or orientation were identified as right hV4, right VO-2, and right V3A/B, which were commonly identified in Experiment 1. The results indicate that these commonly identified visual areas in the human visual cortex may play important roles in glossiness perception.

Introduction

Glossiness is a distinct visual feature that reflects the physical characteristics of object surfaces, or more specifically, surface reflectance properties. Its ecological importance for humans has been investigated from several viewpoints, such as material perception (Adelson, 2001), food freshness perception (Mizrach et al., 2008; Wada et al., 2010), and perception involving social behavior (perception of health and age from human hair: Gangestad and Scheyd, 2005). Humans can judge quite easily whether an object is glossy or matte; however, it is computationally difficult to correctly estimate surface reflectance properties from an object's retinal image. This is because the image intensity (i.e., luminance) depends not only on the surface reflectance properties but also on the light source intensity and the geometrical relationships among the light sources, the surface orientation, and the viewpoint (Bertero et al., 1988; Dror et al., 2001; Horn, 1977; Horn and Sjoberg, 1979; Nicodemus et al., 1977; Pont and te Pas, 2006).

Recent advances in psychophysical studies have revealed that the human visual system uses a variety of different glossiness cues when confronted with the glossiness estimation problem. For instance, specular highlight and reflection of the environment play an important role in glossiness perception (Beck and Prazdny, 1981; Berzhanskaya et al., 2005; Ferwerda et al., 2001; Fleming et al., 2003; Hunter and Harold, 1987; Pellacini et al., 2000). Other studies reported the importance of different properties (luminance contrast of object surface: Ferwerda et al., 2001; Hunter and Harold, 1987; Marlow and Anderson, 2013; Marlow et al., 2012; image statistics: Motoyoshi et al., 2007; highlight color: Nishida et al., 2008, 2011; shape: Anderson and Kim, 2009; Kim et al., 2011; Marlow et al., 2011; binocular cues: Blake and Bülthoff, 1990; von Helmholtz, 1910; Hering, 1964; Hurlbert et al., 1991b; Motoyoshi et al., 2007; Obein et al., 2004; Sakano and Ando, 2010; Wendt et al., 2008, 2010; dynamic cues: Hartung and Kersten, 2002; von Helmholtz, 1910; Hering, 1964; Hurlbert et al., 1991a, b; Sakano and Ando, 2010; Wendt et al., 2010). This psychophysical evidence has suggested that multiple visual features may be involved in glossiness perception, which could further imply that multiple cortical regions responsible for these visual features are recruited in glossiness estimation.

However, despite the implications from these psychophysical studies, the neural correlates of glossiness processing have not been directly measured except for in two recent monkey studies. Nishio et al. (2012) reported selective neural responses to glossy surfaces that were found

Abbreviations: VO, ventral–occipital; CoS, collateral sulcus.

* Corresponding author at: Center for Information and Neural Networks (CiNet), NICT, 1-4 Yamadaoka, Suita, Osaka 565-0871, Japan. Fax: +81 671748612.
E-mail addresses: a-wada@nict.go.jp (A. Wada), yuichi@nict.go.jp (Y. Sakano), h-ando@nict.go.jp (H. Ando).

http://dx.doi.org/10.1016/j.neuroimage.2014.05.001

in monkey inferior temporal (IT) cortex from the results of their single unit recording experiments. Okazawa et al. (2012) used functional magnetic resonance imaging (fMRI) to uncover the activations invoked by glossy surfaces in the monkey visual cortex ranging from the early visual areas to the IT cortex. In the case of humans, however, the involvement of brain regions other than the ventral visual cortex has been suggested. Kentridge et al. (2012) reported in their behavioral results that a visual agnosic patient with ventral occipital lesions was able to discriminate a glossy surface from a matte one. Doerschner et al. (2011), based on their behavioral and computational results, suggested a hypothetical neural mechanism possibly in MST in the dorsal visual cortex using three motion cues for estimating surface reflectance properties, which well explained both successes and failures of glossiness estimation in humans. These results appear somewhat contradictory to those of the monkey studies that reported the neural correlates of glossiness processing in the ventral visual cortex, and thus raise the question of which cortical regions in the human visual cortex are involved in glossiness processing. However, neither Kentridge et al. nor Doerschner et al. directly addressed this question in their study because they performed no direct measurement of the neural activity. In the literature on the neural processing of object surface properties, neuroimaging studies used visual stimuli consisting of objects with different glossiness levels (texture: Cant and Goodale, 2007; Cant et al., 2009; material properties: Cant and Goodale, 2011; Hiramatsu et al., 2011; shape from texture and shading: Georgieva et al., 2008). However, their main focus was not on glossiness, and thus neural correlates were not specifically examined.

In this study, we carried out the first human neuroimaging experiments that directly investigated the neural correlates of glossiness perception. Our main objective is to identify where in the human visual cortex the processing of glossiness resides, or more specifically, whether and how each of the ventral and dorsal visual pathways (Goodale, 1992; Milner and Goodale, 2006; Ungerleider and Mishkin, 1982) play a role in the estimation of glossiness. A difficult issue here in identifying possible glossiness processing regions is that, as implied by psychophysical evidence that a variety of visual features affect perceived glossiness, we might find glossiness processing regions to be distributed throughout the visual cortex rather than localized in a single functional area. In this case, it would be difficult to tell whether each one of the identified regions is processing one of multiple glossiness cues or further playing a central role in the processing of glossiness that might give rise to glossiness perception. To cope with this issue, we used two experimental paradigms for different aims to investigate the neural substrates of glossiness perception. In Experiment 1, we used a paradigm based on stimulus-induced response, which simply compared the neural responses to visual surfaces with high and low glossiness. By using this stimulus-based paradigm, we aimed at inclusively identifying possible glossiness processing regions induced by high vs. low glossiness while the visual system is actively engaged in glossiness discrimination, which may include those that process cues for glossiness but that do not necessarily play a central role in glossiness processing. As specular highlights on glossy surfaces typically increase luminance magnitude and the luminance contrast, we controlled them in the stimulus images using an illumination factor with bright and dim levels of illumination. By introducing this control, we aimed at dissociating the neural response induced by glossiness from that by each of these elementary visual features, which is reported to evoke neural responses by itself in the human visual cortex, especially in V1 (luminance magnitude: Horiguchi et al., 2009; luminance contrast: Avidan et al., 2002; Boynton et al., 1996, 1999; Gardner et al., 2005; Hall et al., 2005; Heeger et al., 2000; Logothetis et al., 2001; Olman et al., 2004; Tootell et al., 1995). If a cortical region showed higher neural responses for high glossiness stimuli than for low glossiness stimuli regardless of the differences in illumination level, such regions are probably involved in the processing of glossiness. Furthermore, this stimulus-based paradigm, when combined with a psychophysical rating of glossiness, enabled us to examine direct correlations between the stimulus-induced neural response and its corresponding percept. In Experiment 2, we adopted a paradigm based on attention-induced response modulation, which has been reported to be successful for identifying the region specialized for processing the attended feature (Liu et al., 2003) with several examples (Cant and Goodale, 2007; Cant and Goodale, 2011; Corbetta et al., 1990; Murray and Wojciulik, 2004). By using this paradigm, we aimed at conservatively identifying cortical regions that play a central role in glossiness processing, which might give rise to glossiness perception. The subjects were forced to direct their attention selectively to glossiness, 3D form, or orientation, which was achieved by instructing them to discriminate whether a paired stimulus objects differed or not in the specified feature. If certain areas are more activated in the glossiness discrimination condition than either of the other conditions, such results may suggest that these areas are modulated by attention to glossiness, and thus might be playing a central role in glossiness processing. Furthermore, this attention-based approach enabled complete control over possible bottom-up responses to any confounding visual feature with glossiness. We achieved this by keeping the set of stimuli identical across all three experimental conditions mentioned above (i.e., glossiness, 3D form, and orientation), thus assuring that the measured effects were due solely to attentional modulation. We expected that the combination of these two different approaches would allow us to obtain comprehensive and reliable results regarding the neural correlates of glossiness perception, because Experiment 1 may inclusively identify regions related to glossiness processing and Experiment 2 may conservatively localize regions for central processing of glossiness.

In both experiments, in addition to conventional statistical parametric mapping (SPM) analysis, we applied region of interest (ROI) analysis to multiple visual areas. Based on recent findings regarding visual field maps in humans, we ran a retinotopic mapping localizer to segregate the following visual areas in the striate and extrastriate visual cortex: V1, V2, V3, hV4, VO-1, VO-2, LO-1, LO-2, V3A/B, and V7. Using retinotopically defined ROIs, we avoided the spatial uncertainty introduced by intersubject or interhemispheric variability of the anatomical location of human visual areas. We also included in our analysis a motion sensitive area, hMT+, which is defined by a conventional motion localizer, and two individually defined anatomical regions, the collateral sulcus (CoS) and the intraparietal sulcus (IPS). These 13 ROIs covering the ventral and dorsal visual pathways enabled a more precise and comprehensive examination of the processing of glossiness in the human visual cortex.

Material and methods

Subjects

All three of the authors and nine naive volunteers (eight males and four females, 25–49 years of age, mean 36.7) participated in Experiment 1, and all three of the authors and 10 volunteers (10 males and three females, 26–49 years of age, mean 35.2) participated in Experiment 2. All subjects were healthy, with normal or corrected-to-normal vision, and no history of neurological disorders. All subjects were experienced in keeping still and maintaining fixation during fMRI experiments. The subjects gave written informed consent for the experimental procedures approved by the ATR Human Subject Review Committee (Keihanna Science City, Kyoto). In Experiment 2, three subjects were excluded from the analyses because their head motion exceeded the voxel size of 3 mm within an experimental run (one male) or because the average task performance did not reach 95% in one or more of the experimental conditions (one male and one female).

Apparatus

The stimuli were shown with Presentation (Neurobehavioral Systems, Albany, Canada) on a personal computer and back-projected by a DLP projector (DLA-G150CL; JVC, Yokohama, Japan) onto a translucent screen. The subjects viewed them on the screen by way of an

oblique mirror mounted on the head coil. The projector's spatial resolution was 1024 × 768 pixels (18° × 13.5° in visual angle), and the refresh rate was 60 frames per second. The minimum and maximum luminances were 0.029 cd/m^2 and 106.77 cd/m^2, respectively. The distance from the subjects' eyes to the screen was 110 cm. The visual acuity of the subjects with refractive errors was corrected by using MRI-compatible plastic lenses. Responses were obtained using a two-button fMRI-compatible response pad (Fiber Optic Response Pad, Current Designs, Philadelphia, PA, USA), where the subjects made responses with their right thumb by pressing one of those two buttons.

Stimuli

Retinotopic mapping localizer stimuli

We used a standard retinotopic mapping localizer to identify different visual areas in the cortex, where the subjects passively viewed flickering checkerboard stimuli configured in a rotating wedge and an expanding or contracting ring to derive the polar angle and eccentricity maps, respectively (Engel et al., 1994; Wandell et al., 2007; Warnking et al., 2002). Dark and light checks were reversed, and the chromaticity was randomly reassigned at a 4-Hz flicker frequency. We alternated between clockwise and counterclockwise rotations for the wedge stimuli or expansion and contraction for the ring stimuli on subsequent runs. The polar angle wedge was 45° wide and extended to the edges of the screen. The periodicity of both types of stimuli was 32 s (12 cycles per run). During eccentricity mapping, the ring increased logarithmically as a function of time in both the size and rate of expansion, based on human cortical magnification. The ring's duty cycle was 25%. In each scanning run, the subjects fixated on a small (≈8 arcmin) dot in the center of the screen. To help maintain arousal and concentration, the subjects were instructed to press a button whenever the fixation point's color changed from green to red. This color-changing event occurred at random intervals throughout the scan, every 4.5 s on average. This retinotopic mapping localizer consisted of two runs of eccentricity mapping using an expanding/contracting ring and four runs of polar angle mapping using clockwise/counter-clockwise rotating wedges for each subject.

Motion localizer stimuli

The locations of hMT+ (Tootell et al., 1995; Watson et al., 1993; Zeki et al., 1991) were functionally identified based on stimuli responses that alternated between moving and stationary dot patterns, with durations of 27 and 9 s, respectively. The hMT+ localizer used here resembled that used in Huk et al. (2002) and Amano et al. (2009). Moving dots traveled toward and away from the fixation point (8°/s), which extended to the edges of the screen, altering direction every second (white 0.25° diameter dots on a black background). Two runs of this hMT+ localizer were carried out for each subject; each run consisted of eight cycles of the motion and stationary patterns.

Experimental stimuli

The stimuli consisted of a series of unfamiliar red objects placed on a checkerboard ground with a blue sky-like background generated by computer software (3ds Max; Autodesk, San Rafael, CA, USA), where the eccentricity of the objects was in the range of 0–7.43° at maximum. The objects were simulated to be illuminated by parallel white light from above the observer's head at a 45° elevation angle. This scene setup included multiple glossiness cues in the stimuli, which normally exist under natural conditions. The resulting stimuli provided rich information on surface glossiness, including specular highlights and reflections of the environment (Beck and Prazdny, 1981; Berzhanskaya et al., 2005; Ferwerda et al., 2001; Fleming et al., 2003; Hunter and Harold, 1987; Pellacini et al., 2000) as well as differences in the spectral distribution between specular and diffuse reflections (Nishida et al., 2008, 2011). The existence of multiple cues helps produce obvious glossiness (Nishida and Shinya, 1998; Wendt et al., 2008, 2010; Sakano and Ando, 2010).

In Experiment 1, we manipulated three independent visual features of the stimulus: glossiness (four levels), the object's 3D form (four types), and the illumination level (bright or dim). The higher (3 and 4) or lower (1 and 2) pair of glossiness levels was assigned to high or low glossiness conditions, respectively; this procedure is described in detail later in the Experimental procedures section. Stimuli with all 32 possible combinations of visual features were used in the experiment (Fig. 1). Glossiness was modulated by setting the 3ds Max rendering parameters, including those that changed the Phong exponent (Phong, 1975), and the specular and diffuse reflectances (see Supporting Information for details). For glossiness levels of 4 (highest) or 1 (lowest), these parameter values were adjusted to generate glossy or matte appearances. For glossiness levels of 2 and 3, each of these parameter values was decided by linear interpolation among the parameter values of the glossiness levels of 1 and 4. Available glossiness cues in the resulting images included the specular highlights and reflections of the checkerboard ground. The illumination level was modulated by setting the intensity parameters of the sun and sky simulators in 3ds Max (see Supplementary Methods for details).

In order to control luminance magnitude and luminance contrast, which typically co-vary with glossiness, we set the illumination level for each bright and dim conditions so that the effect of the illumination factor on the luminance magnitude and the luminance contrast became stronger than that of the glossiness factor. More specifically, the values of the rendering parameters related to illumination were adjusted (see Supplementary Methods for details) so that the mean luminance within the object and over the entire image would be higher under the bright compared with the dim illumination level; the different illumination levels caused larger differences in mean luminance than the different glossiness levels do (Fig. 2). Consequently, the images' luminance root-mean-square (RMS) contrast, which we defined as a pixel-wise standard deviation of luminance divided by the mean of entire image (Olman et al., 2004), resulted in a similar profile to that of the mean luminance[1] and thus met the requirements for the experimental control described above (Fig. 2).

An identical set of stimuli was used in the rating experiment, where the perceived glossiness for each stimulus was psychophysically measured. The standard stimulus was the X-like object with the highest glossiness rendered under the bright illumination (the image marked with a green box in Fig. 1).

In Experiment 2, we manipulated three different feature dimensions: glossiness (glossy or matte), 3D form (O-like or X-like), and the object's 3D orientation (left or right side closer to the subject) (Fig. 3). To manipulate the glossiness level, we derived a set of parameter values from Experiment 1 to render object surfaces, where glossiness levels of 4 and 1 were applied to the glossy and matte surfaces, respectively. Two object forms were also derived from Experiment 1. We used all eight possible combinations of visual features in the experiment.

Experimental procedures

In all experiments, the subjects fixated on the fixation crosses or circles when they were presented at the center of the screen. When neither was presented, they fixated on the center of the screen.

Experiment 1: stimulus-induced neural response

We used an event-related design to measure the fMRI response to the effect of the glossiness (high vs. low) and illumination (bright vs. dim) factors. These two factors were combined to form the following

[1] A difference in illumination intensity does not, in theory, affect the scene's luminance contrast (Vladusich et al., 2006). However, as the rendering software we used does not perform a physically correct simulation of light transport, we consider that the effect of illumination level on the RMS contrast found in our stimulus images may have been introduced by the physically inaccurate luminance calculation, which might be specific to the implementation of the rendering effects in the software we used.

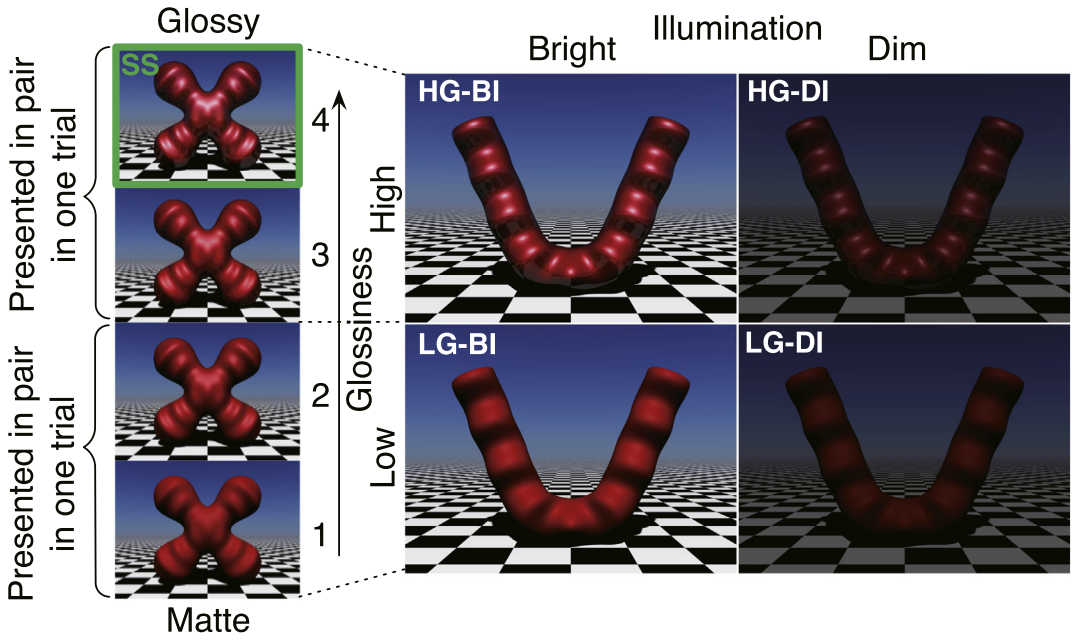

Fig. 1. Examples of stimuli used and experimental conditions designed for Experiment 1. A series of unfamiliar red objects was generated on a checkerboard ground with a blue sky-like background. Three independent visual features, glossiness (four levels), 3D form (four types), and illumination level (bright or dim), were manipulated. For the experimental conditions, two factors, glossiness and illumination, were combined to form the following four conditions: high glossiness under bright illumination (HG-BI), low glossiness under bright illumination (LG-BI), high glossiness under dim illumination (HG-DI), and low glossiness under dim illumination (LG-DI). A pair of images with glossiness levels of 1 and 2 or 3 and 4 was presented in one trial under high- or low-glossiness conditions, respectively. The standard stimulus (SS) used in the rating experiment is marked by a green box, which was the X-like object with the highest glossiness rendered under the bright illumination.

four experimental conditions: high glossiness under bright illumination (HG-BI), low glossiness under bright illumination (LG-BI), high glossiness under dim illumination (HG-DI), and low glossiness under dim illumination (LG-DI) (Fig. 1). In each trial, paired stimuli were presented sequentially for 2.5 s for each with a 2-s ISI and a 2-s blank after the second stimulus (Fig. 4). Each pair consisted of two stimuli whose glossiness levels were 1 and 2 for the high glossiness conditions (HG-BI and HG-DI) or 3 and 4 for the low glossiness conditions (LG-BI and LG-DI), where possible combination of glossiness level and object form attributed to each pair were counterbalanced across trials for each of the four experimental conditions. The subjects judged which stimulus appeared glossier and pressed the corresponding button as soon as the second stimulus ceased. The number of button presses when correctly answered was counterbalanced across the buttons, where the left or right button press indicated that the first or second stimulus was glossier than the other, respectively. Thirty-two trials were conducted in a run. For each subject, 10 runs were conducted. The trial order was randomized and counterbalanced across runs, where each of the 32 stimulus images was presented 10 times across runs for each subject.

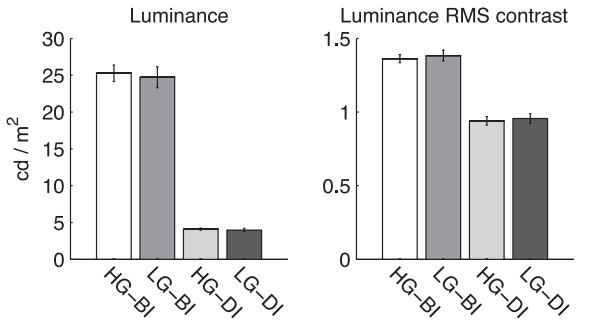

Fig. 2. Image statistics of stimulus images in Experiment 1. Mean luminance and RMS luminance contrast were calculated for each of four experimental conditions: high glossiness under bright illumination (HG-BI), low glossiness under bright illumination (LG-BI), high glossiness under dim illumination (HG-DI), and low glossiness under dim illumination (LG-DI). Both statistics showed higher values under bright illumination conditions than under dim illumination conditions (HG-BI vs. HG-DI and LG-BI vs. LG-DI), but no significant differences were found between high- and low-glossiness conditions (HG-BI vs. LG-BI and HG-DI vs. LG-DI).

Experiment 2: attention-induced response modulation

We used a block design to measure the fMRI response differences among attending to glossiness, form, and object orientation. The design was adapted from Cant and Goodale (2007). Fixation and instruction periods preceded experimental blocks (Fig. 5). Each block had eight trials, each of which lasted 2 s. In each trial, the paired stimuli were presented sequentially for 0.6 s and interleaved with 0.2-s intervals. The subjects judged whether the paired stimuli were the same in terms of the instructed visual feature (i.e., glossiness, form, or object orientation) and pressed the corresponding button as soon as the second stimulus ceased. The sequence of fixation and instruction periods and an

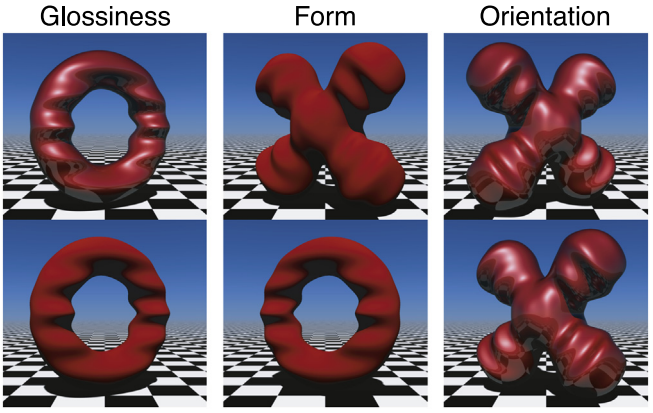

Fig. 3. Examples of stimuli used in Experiment 2. Three independent visual features were manipulated: glossiness, form, and orientation. Two different levels of glossiness, glossy and matte, were shown on the same object in the same orientation (left). Two different forms were shown with the same glossiness level in the same orientation (middle). Two different orientations were shown with the same glossiness level and form (right).

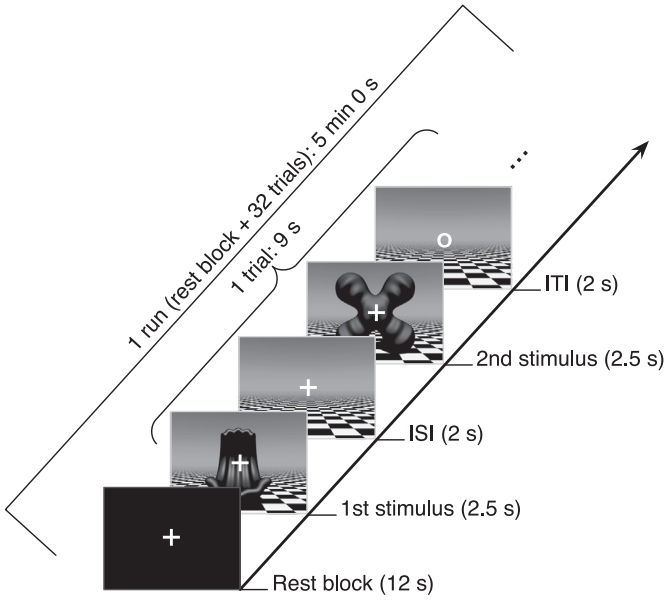

Fig. 4. Protocol used in Experiment 1. In each experimental trial, a pair of stimulus images was presented, followed by an inter-trial interval (ITI) where subjects responded to glossiness judgment tasks. A rest block was placed at the beginning of each run.

experimental block were repeated 12 times. Eight runs were conducted for each subject. The block order was randomized and counterbalanced across subjects and runs.

Rating experiment

We performed a psychophysical experiment to measure the perceived glossiness of each stimulus presented in Experiment 1. In this experiment, we used the same experimental apparatus as in Experiment 1 but did not perform the magnetic resonance examinations. At the beginning of each run, the standard stimulus was presented once for 2.5 s, which was followed by the sequence of target stimuli whose presentation time course was identical with those in Experiment 1. The standard stimulus was the X-like object with the highest glossiness under the bright illumination (the image marked with a green box in Fig. 1). The subjects verbally reported the perceived glossiness of each stimulus by giving a number based on the assumption that the glossiness of the standard stimulus was 10. Zero meant no perceived glossiness: completely matte. Each verbal report was completed before the next stimulus was presented. Five runs were conducted for each subject, where each run consisted of 64 stimulus presentations.

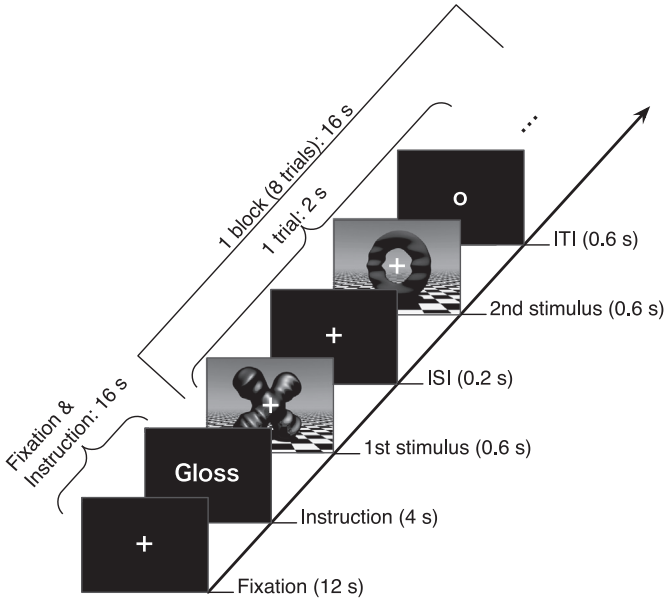

Fig. 5. Protocol used in Experiment 2. Experimental blocks were interleaved with fixation periods. After presentation of each fixation block, an instructional cue was presented, where participants directed attention to a particular stimulus dimension.

Magnetic resonance imaging data acquisition

Magnetic resonance (MR) examinations were performed using a 3-T MR scanner (Siemens TIM Trio; Siemens Medical Systems, Erlangen, Germany) equipped with a 12-channel head coil. Single-shot echo-planar imaging (EPI) images were collected whose slice orientation was parallel to the anterior commissure–posterior commissure line except for the retinotopic mapping localizer scans, where the slices were approximately oriented parallel to the calcarine fissure. We used the following pulse sequence parameters: 2000 ms repetition time (TR), 30 ms echo time (TE), 80° flip angle (FA), in-plane voxel size of 3×3 mm, 3-mm-thick slices, matrix size of 64×64, and 30 slices covering the entire occipital cortex and the posterior parts of the temporal and parietal cortices.

A pair of T1-weighted anatomical images (magnetization prepared rapid gradient echo) was acquired for each subject for spatial normalization in the preprocessing steps, visualization in the SPM analysis, and the cortical surface extraction. The following were the pulse sequence parameters: TR, 2250 ms; TE, 3.06 ms; FA, 9°; voxel size, $1 \times 1 \times 1$ mm; matrix size, 64×64; and 192–208 sagittal slices covering the whole head.

To aid accurate mapping between the anatomical and functional images, high in-plane resolution T2-weighted images (turbo spin echo) were acquired for each subject, whose field of view, slice thickness, number of slices, and slice orientation were identical with those of the functional EPI images. The following were the pulse sequence parameters: TR, 6000 ms; TE, 57 ms; FA, 160°; voxel size, $0.75 \times 0.75 \times 3$ mm; and matrix size, 256×256.

Data analysis

We analyzed the data using multiple types of software. The SPM analysis for Experiments 1 and 2 was performed using SPM8. The ROI analysis for Experiments 1 and 2 was performed with a MarsBar toolbox. The ROI masks were created using multiple software packages: SPM8 and the MarsBar toolbox were used to localize hMT+, and the FreeSurfer and FS-Fast software suites were used to identify both the retinotopically defined visual areas (V1, V2, V3, hV4, VO-1, VO-2, LO-1, LO-2, V3A/B, and V7) and the anatomically defined regions (CoS and IPS). We applied the following preprocessing steps to the functional EPI images: slice-timing correction, motion correction, normalization to the Montreal Neurological Institute (MNI) stereotaxic space, and spatial smoothing using a Gaussian kernel with a 6-mm full width at half maximum. For preprocessing of the retinotopic mapping localizer, spatial smoothing and normalization were not applied. The statistical tests used in the ROI and behavioral analyses were done with SPSS (SPSS Inc., Chicago, IL, USA).

Region of interest localization

The ROIs that were used later in the ROI analysis section were localized based on the two types of MRI data: the functional images acquired from the retinotopic and motion localizer experiments, and the structural images that gave detailed anatomy of the subjects' brains. The analyses were performed on the eight subjects that participated in the both localizer experiments (eight subjects each for Experiment 1 and 2).

Using the retinotopic localizer data, the 10 visual areas (V1, V2, V3, hV4, VO-1, VO-2, LO-1, LO-2, V3A/B, and V7) were localized. Each boundary between adjacent visual areas was demarcated based on the visual field maps for the two retinotopic representations: polar angle representation derived from the rotating wedge stimuli and eccentricity

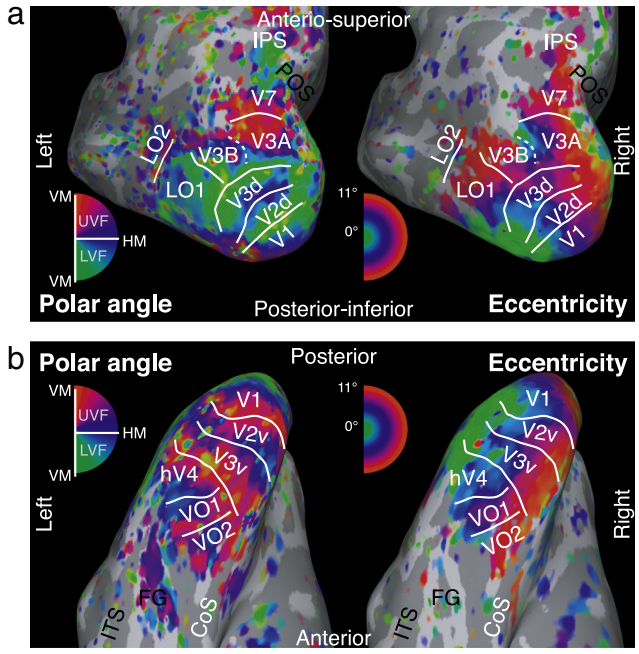

Fig. 6. Results of retinotopic mapping localizer for one subject. Multiple visual field maps were segregated based on two phase maps derived from localizer experiment: (a) polar angle representation and (b) eccentricity representation. Preferred polar angle in the contralateral hemifield and eccentricity are represented by different colors (in the range of green to red) as indicated by the color wheel key. IPS, intraparietal sulcus; POS, parieto-occipital sulcus; CoS, collateral sulcus; FG, fusiform gyrus; OTS, occipitotemporal sulcus; LH, left hemisphere; RH, right hemisphere; VM, vertical meridian; HM, horizontal meridian.

representation derived from the expanding or contracting ring stimuli, respectively. To clearly visualize the retinotopic organization in the visual cortex, these maps were projected onto the inflated individual cortical surface extracted from the anatomical images of the corresponding subject. Each example of the polar angle and eccentricity maps was shown in Fig. 6, which was estimated from one subject. The visual areas were segregated and labeled by following the definition and notation of Wandell et al. (2007). The primary visual area, V1, was identified around the occipital pole and the calcarine sulcus. The dorsal and ventral parts of V2 and V3 were also identified (V2d, V3d, V2v, and V3v), which occupy a strip of cortex that encircles V1. The visual areas that mainly constitute the ventral visual cortex, hV4, VO-1, and VO-2, were identified in the ventral occipital (VO) cortex (Fig. 6b). hV4 was located adjacent to V3v. VO-1 and VO-2 (Brewer et al., 2005; Larsson and Heeger, 2006; Liu and Wandell, 2005) were identified anterior to hV4 and extended to the peripheral representation of V3v (Larsson and Heeger, 2006). Fig. 6a depicts the visual areas that mainly constitute the dorsal visual cortex. In the dorsal direction, V3A/B and V7 were identified, neighboring the peripheral representation of V3d and located around the transverse occipital sulcus (TOS) (DeYoe et al., 1996; Larsson and Heeger, 2006; Tootell et al., 1997; Smith et al., 1998; Swisher et al., 2007). In the lateral direction, LO-1 and LO-2 were identified, neighboring the central representation of V3d and located in the lateral occipital (LO) cortex (Larsson and Heeger, 2006; Swisher et al., 2007). Amano et al. (2009) reported that the location known as the lateral occipital complex (Grill-Spector and Malach, 2004; Malach et al., 1995) mainly corresponds with LO-2. Because the lateral occipital region is well known to play a significant role in the processing of objects (Kourtzi and Kanwisher, 2000; Malach et al., 1995), it has been conventionally categorized into the ventral visual pathway. We followed this convention and categorized LO-1 and LO-2 into the ventral visual cortex in this study. Amano et al. (2009) also showed two visual field maps, TO-1 and TO-2, that border LO-2 anteriorly in the temporal occipital (TO) cortex whose location corresponds with motion-sensitive area hMT+. Instead of localizing TO-1 and TO-2, which, as previously reported (Amano et al., 2009), were difficult to reliably identify retinotopically with standard visual field mapping localizer and analysis, we used a conventional motion localizer.

We localized hMT+ by contrasting the motion and stationary conditions in the motion localizer, the analysis procedure of which was basically identical to that of the SPM analysis for the main experiments described in the following subsection. The significance threshold was set between $p = 0.005$ and $p = 0.00005$; the exact value was decided to delineate a distinct cluster corresponding to hMT+. We confirmed that the localized cluster resided anterior to the identified LO-1/2.

From the structural MRI data, we prepared two anatomically defined regions, the collateral sulcus (CoS) and the intraparietal sulcus (IPS), which was performed on an individual subject basis using FreeSurfer's automatic segmentation algorithms.

In the current study, the above 13 ROIs were categorized into three groups: the early visual cortex, which includes V1, V2, and V3; the ventral visual cortex, which includes hV4, VO-1, VO-2, CoS, LO-1, and LO-2; and the dorsal visual cortex, which includes V3A/B, V7, IPS, and hMT+.

SPM analysis

We performed SPM analysis based on conventional general linear model (GLM) analysis using SPM8, including in the model the six-dimensional motion regressors that were derived from the motion correction step in the preprocessing procedures.

For Experiment 1, the following four experimental conditions were modeled as four GLM regressors: HG-BI, LG-BI, HG-DI, and LG-DI. The time course of each regressor was modeled with the corresponding stimulus presentation time periods. Based on the regression coefficients derived from the GLM analysis, we examined the positive main effect of glossiness, which compared the high and low glossiness conditions (HG-BI and HG-DI vs. LG-BI and LG-DI), and the positive main effect of illumination, which compared the bright and dim conditions (HG-BI and LG-BI vs. HG-DI and LG-DI). The interaction between the glossiness and illumination factors was also examined (HG-BI and LG-DI vs. LG-BI and HG-DI).

For Experiment 2, attention to each of the glossiness, form, and orientation conditions was modeled as an independent GLM regressor. The neural modulation induced by attention to glossiness was assessed by conjunction analysis, where the activation level of the glossiness condition was contrasted with either the form or orientation condition. Cortical regions that elicited activation in either contrast (glossiness vs. form or glossiness vs. orientation) were identified as the regions whose neural responses were positively modulated by attention to glossiness. Additionally, each of the modulations induced by attention to form and orientation was investigated by the same procedure.

In the subsequent group analyses for Experiments 1 and 2, we applied an uncorrected peak-level threshold of $p < 0.001$ to the derived activation maps, and performed multiple-comparison correction with the cluster-level false discovery rate (FDR) at a level of $p < 0.05$. For the ease of visualization, the significantly activated clusters were rendered on fsaverage, which is an averaged cortical surface provided by FreeSurfer.

Region of interest analysis

ROI analyses were also performed for each subject to complement the SPM analysis. The following visual fields were functionally defined as ROIs by the retinotopic mapping localizer: V1, V2, V3, hV4, VO-1, VO-2, V3A/B, V7, LO-1, and LO-2. The motion localizer was used to identify hMT+. Additionally, we used two ROIs in the association cortices, the collateral sulcus (CoS) and the IPS, which were identified as a result of FreeSurfer's cortical surface reconstruction and automatic anatomical labeling procedures. In Experiment 2, the left and right hemispheres were separately analyzed for each of these ROIs, because the SPM analysis results indicated relatively lateralized activation patterns between hemispheres. For each ROI, we extracted the average signal time course

over voxels in that region and applied GLM analysis; the models were identical with those used in the SPM analysis. The resulting contrast estimates were then scaled to the blood-oxygen-level dependence (BOLD) signal changes. For Experiment 1, the BOLD signal changes in all four experimental conditions, the combination of the glossiness (high and low) and illumination (bright and dim) factors, were collected across the experimental runs and the subjects. The main effects of glossiness and illumination with their interactions were examined by performing a two-way repeated-measures analysis of variance (ANOVA) for each ROI, whose procedure was in principle identical with that applied in the corresponding SPM analysis. For Experiment 2, we examined the positive response modulation induced by attention to glossiness. We compared the BOLD signal change of the glossiness condition with that of each of the other two conditions, the form and orientation conditions. ROIs that showed activation in either comparison (glossiness vs. form or glossiness vs. orientation) were identified as the ROIs whose neural responses were positively modulated by attention to glossiness. This procedure basically corresponded to the conjunction analysis applied in the SPM analysis. We also assessed the modulation induced by attention to form (form vs. glossiness or form vs. orientation) and orientation (orientation vs. glossiness or orientation vs. form) by performing the same analysis. The statistical significance was tested using a paired t-test on the ROI basis, which examined the following three comparisons: glossiness vs. form, glossiness vs. orientation, and form vs. orientation. The resulting significance level was Bonferroni corrected by a factor of 3, the number of pairwise comparisons conducted for each ROI.

Behavioral analysis

The behavioral performance (percent accuracy) obtained during the fMRI runs in the scanner was analyzed for both experiments. For Experiment 1, the main effects of glossiness and illumination with their interaction were examined by performing a two-way repeated-measures ANOVA. For Experiment 2, the differences among the three experimental conditions were tested by performing a one-way repeated-measures ANOVA.

The perceived glossiness obtained from the rating experiment was similarly analyzed. We grouped the rating scores by experimental condition for each subject and entered them into a two-way repeated-measures ANOVA. The main effects of glossiness and illumination with their interaction were examined.

Correlation analysis

The perceived glossiness and image statistics of the stimulus images were investigated to determine their relationship with the neural responses for each ROI. The scale of the BOLD signal changes for the four experimental conditions was z-score normalized for each subject and then collected across the eight subjects in the ROI analysis. The rating scores of the perceived glossiness for all 32 stimulus images were grouped into four sets that corresponded to the four experimental conditions (HG-BI, LG-BI, HG-DI, and LG-DI) and averaged within each set for each subject, which were further z-score normalized and collected across subjects. Pearson's correlation coefficient was computed by comparing the normalized BOLD signal changes and the normalized rating score derived above. For each of the two image statistics, mean luminance and luminance RMS contrast, we computed the correlation to the normalized BOLD signal change using the same procedure as for the rating score.

Results

Experiment 1: stimulus-induced neural response

The main effects of glossiness, which compared the high and low glossiness conditions (HG-BI and HG-DI vs. LG-BI and LG-DI), and the main effect of illumination, which compared the bright and dim conditions (HG-BI and LG-BI vs. HG-DI and LG-DI), were investigated for stimulus-induced neural response in the visual cortex. The interaction between the glossiness and illumination factors (HG-BI and LG-DI vs. LG-BI and HG-DI) was also examined.

SPM analysis

We identified five clusters of activation by SPM analysis, which met the criteria of cluster-level FDR control (Table 1). For the positive main effect of glossiness, we identified a bilateral pair of clusters that covered a broad region in the occipital cortex along the ventral and dorsal visual pathways. Fig. 7a illustrates the approximate regions covered by these clusters, which extended from the ventral occipital area, including the posterior part of the fusiform gyrus (FG), to the superior occipital area, including the TOS. For the positive main effect of illumination, we identified a bilateral pair of clusters in the calcarine fissure (Fig. 7b). For the interaction between glossiness and illumination, the regions covered by the bilaterally identified significant clusters largely overlapped those of the main effect of glossiness, which extended from the ventral occipital area that included the posterior part of the FG to the superior occipital area (Fig. 7c).

ROI analysis

For the eight subjects that underwent the retinotopic and motion localizers, the precise activation profile for each visual area was examined on an ROI basis. The BOLD signal changes were averaged across subjects for each of the four experimental conditions (HG-BI, HG-LI, LG-BI, and LG-DI), which was the combination of glossiness (high and low) and illumination (bright and dim) factors (Fig. 8). A two-way repeated-measures ANOVA was applied to these BOLD signal changes to test the main effects of the glossiness and illumination factors and their interaction (Table 2). The ROIs that showed glossiness-specific responses were identified as V2, V3, hV4, VO-1, VO-2, CoS, LO-1, and V3A/B, where we found a significant main effect of glossiness (V2: $F_{1,7} = 7.87$, $p = 0.026$; V3: $F_{1,7} = 15.76$, $p = 0.0054$; hV4: $F_{1,7} = 20.17$, $p = 0.0028$; VO-1: $F_{1,7} = 8.74$, $p = 0.021$; VO-2: $F_{1,7} = 6.25$, $p = 0.041$; CoS: $F_{1,7} = 9.63$, $p = 0.017$; LO-1: $F_{1,7} = 26.16$, $p = 0.0014$; and V3A/B: $F_{1,7} = 15.32$, $p = 0.0058$). In these ROIs, the sign of the effect was positive (high vs. low glossiness), and thus we found no ROI that showed a significant negative

Table 1
Results of SPM analysis of Experiment 1, averaged across 12 subjects. Clusters of statistically significant contiguous activation were identified (FDR-corrected $p < 0.05$, cluster level).

Region name	Laterality	Peak MNI coordinate			Peak value	Cluster size
		x	y	z	(Z-score)	(# voxels)
(a) Positive main effect of glossiness						
Middle occipital, inferior occipital, lingual, and fusiform gyri	(R)	34	−66	−8	6.43	1918
Middle occipital, inferior occipital, lingual, and fusiform gyri	(L)	−28	−78	−10	5.74	1907
(b) Positive main effect of illumination						
Calcarine fissure	(LR)	0	−84	−4	4.99	768
(c) Interaction between glossiness and illumination						
Middle occipital, inferior occipital, lingual, and fusiform gyri	(L)	−28	−94	8	4.97	903
Inferior occipital, lingual, and fusiform gyri	(R)	30	−64	−2	4.46	415

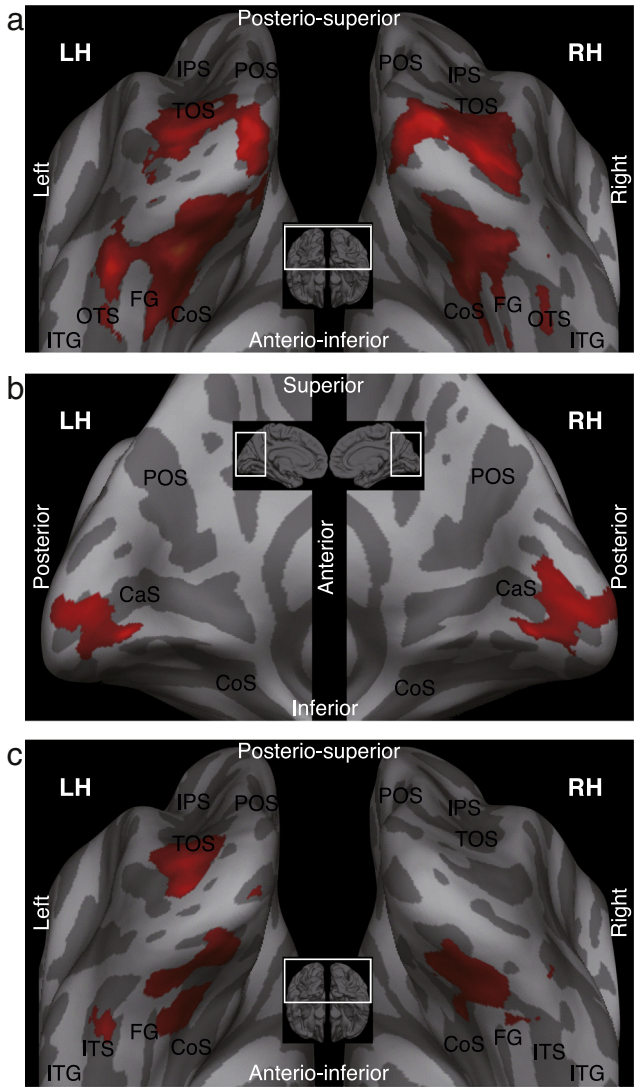

Fig. 7. Results of SPM analysis of Experiment 1, averaged across 12 subjects. Significantly activated clusters identified by SPM analysis were rendered on fsaverage, an averaged cortical surface provided with FreeSurfer (FDR-corrected $p < 0.05$, cluster level). (a) positive main effect of glossiness factor (high vs. low). (b) positive main effect of illumination factor (bright vs. dim). (c) interaction between glossiness and illumination factors. IPS, intraparietal sulcus; TOS, transverse occipital sulcus; POS, parieto-occipital sulcus; CoS, collateral sulcus; FG, fusiform gyrus; OTS, occipitotemporal sulcus; ITG, inferior temporal gyrus; LH, left hemisphere; RH, right hemisphere.

main effect of glossiness (low vs. high glossiness). These ROIs elicited no significant main effect of illumination, and showed a significant positive interaction between glossiness and illumination (V2: $F_{1,7} = 19.17$, $p = 0.0032$; V3: $F_{1,7} = 19.54$, $p = 0.0031$; hV4: $F_{1,7} = 10.94$, $p = 0.013$; VO-1: $F_{1,7} = 21.15$, $p = 0.0025$; VO-2: $F_{1,7} = 11.56$, $p = 0.011$; CoS: $F_{1,7} = 7.35$, $p = 0.030$; LO-1: $_{1,7} = 11.97$, $p = 0.011$; and V3A/B: $F_{1,7} = 15.77$, $p = 0.0054$). The locus of these ROIs well matched the bilateral regions identified by the corresponding SPM analysis, which extended from the ventral occipital area, including the posterior part of the FG, to the superior occipital area, including the TOS. The ROI that showed a response specific to different illumination conditions was identified as V1, where we found a significant main effect of illumination factor ($F_{1,7} = 16.0$, $p = 0.0052$) but no significant main effect of glossiness nor an interaction between glossiness and illumination. This result matched with the pair of bilateral clusters in the calcarine fissure identified by SPM analysis. In the other ROIs, LO-2, V7, IPS, and hMT+, we found no significant effects.

One might suppose that the results shown above could be affected by the neural response to the background scene. As the retinotopic ROIs used were defined on the entire image region in the visual field including both the object surface and the background scene, the voxels that comprise an ROI might have included those corresponding not only to the object surface but also to the background scene. In such case, the neural response might have been affected by the background scene, which differs between different illumination levels. However, our additional analysis that restricted each ROI to the voxels corresponding to the object regions resulted in similar response patterns compared with the original ones (see Supplementary Analysis 1). Thus, it is unlikely that the derived results were merely due to such background effect.

Behavioral analysis

The behavioral task performance (percent accuracy) during fMRI measurements for each of the four experimental conditions (HG-BI: mean [M] = 85.8, standard error of mean [SEM] = 3.96; LG-BI: M = 93.8, SEM = 3.77; HG-DI: M = 85.0, SEM = 2.38; and LG-DI: M = 88.9, SEM = 4.38) was subjected to a two-way repeated-measures ANOVA. Significant main effects of glossiness ($F_{1,11} = 9.40$, $p = 0.010$) and illumination ($F_{1,11} = 5.913$, $p = 0.033$) were shown. No interaction between glossiness and illumination ($F_{1,11} = 1.19$, $p = 0.298$) was found. In conjunction with the preceding section (ROI analysis section), we discuss in Supplementary Discussion 2 that there is unlikely to be a confounding effect of attention on the results of the ROI analysis.

The rating scores for the perceived glossiness were grouped by each of the four experimental conditions for each subject and averaged

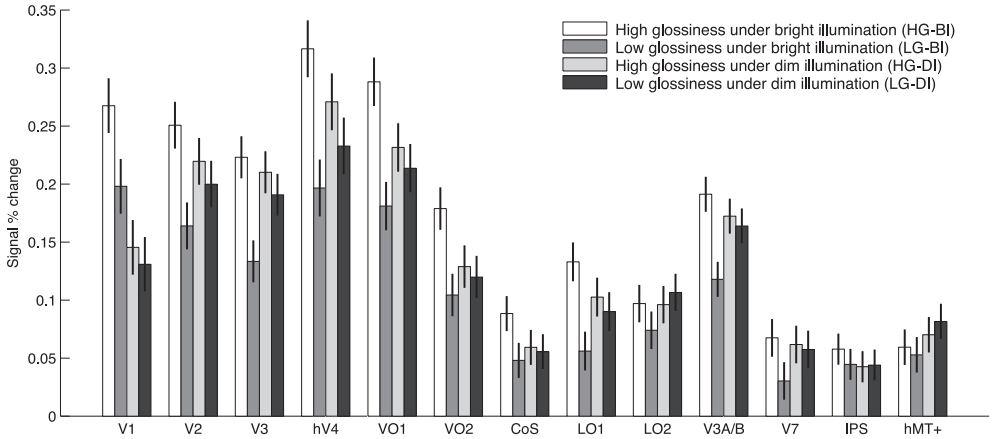

Fig. 8. Results of ROI analysis of Experiment 1. BOLD signal percent change was averaged across eight subjects and compared between different levels of glossiness (high and low) under different levels of illumination (bright and dim). Error bars indicate SEMs.

Table 2
Results of ROI analysis of Experiment 1, averaged across eight subjects. Two-way repeated-measures ANOVA revealed statistical significance for main effects and interaction of glossiness and illumination factors in p- and F-values for each ROI.

ROI	Main effects of glossiness		Main effects of illumination		Interaction	
	p-Value	F-value	p-Value	F-value	p-Value	F-value
V1	0.067^{+}	4.70	0.005**	16.00	0.056^{+}	5.22
V2	0.026*	7.87	0.880	0.02	0.003**	19.17
V3	0.005**	15.76	0.187	2.14	0.003**	19.54
hV4	0.003**	20.17	0.778	0.09	0.013*	10.94
VO-1	0.021*	8.74	0.461	0.61	0.002**	21.15
VO-2	0.041*	6.25	0.355	0.98	0.011*	11.56
CoS	0.017*	9.63	0.258	1.52	0.030*	7.35
LO-1	0.001**	26.16	0.915	0.01	0.011*	11.97
LO-2	0.476	0.57	0.228	1.74	0.115	3.23
V3A/B	0.006**	15.32	0.264	1.47	0.005**	15.77
V7	0.074^{+}	4.41	0.324	1.13	0.064^{+}	4.83
IPS	0.605	0.29	0.163	2.42	0.338	1.06
hMT+	0.781	0.08	0.132	2.90	0.359	0.96

$^{+}$ $p < 0.1$ (tendency).
* $p < 0.05$.
** $p < 0.01$.

across subjects (HG-BI: mean [M] = 8.08, standard error of mean [SEM] = 0.278; LG-BI: M = 3.34, SEM = 0.357; HG-DI: M = 7.08, SEM = 0.293; and LG-DI: M = 2.81, SEM = 0.343) (Fig. 9). To examine the main effects of glossiness and illumination with their interactions, we conducted a two-way repeated-measures ANOVA and found a significant main effect of glossiness ($F_{1,7} = 10.50$, $p = 0.0142$). Neither the main effect of illumination ($F_{1,7} = 1.02$, $p = 0.347$) nor the interaction between glossiness and illumination ($F_{1,7} = 0.325$, $p = 0.587$) showed significance.

Correlation analysis

Both the perceived glossiness and the image statistics of the stimuli used in Experiment 1 were investigated to determine their relationships with the corresponding neural responses for each ROI. For the perceived glossiness, we measured the rating scores for the level of perceived glossiness and calculated its correlation with the BOLD signal changes for each experimental condition for each subject (Fig. 10 and Supplementary Fig. S5). We found significant positive correlations in V1 ($r = 0.386$, $p = 0.0291$), V2 ($r = 0.557$, $p = 0.000927$), V3 ($r = 0.550$, $p = 0.00111$), hV4 ($r = 0.754$, $p = 0.000001$), VO-1 ($r = 0.636$, $p = 0.000091$), VO-2 ($r = 0.531$, $p = 0.00174$), CoS ($r = 0.533$, $p = 0.00169$), LO-1 ($r = 0.624$, $p = 0.000138$), V3A/B ($r = 0.581$, $p = 0.000494$), and IPS ($r = 0.361$, $p = 0.0423$), which largely overlapped with the ROIs identified in the preceding ROI analysis that showed glossiness-specific neural responses: V2, V3, hV4, VO-1, VO-2, CoS, LO-1, and V3A/B. For the image statistics, mean luminance and RMS luminance contrast of each stimulus image were computed and their correlation with the BOLD signal changes was calculated (Fig. 11 and Supplementary Fig. S6). In V1, we found significant positive correlations with mean luminance ($r = 0.584$, $p = 0.00045$) and luminance RMS contrast ($r = 0.564$, $p = 0.000785$). In LO-2 and hMT+, we found significant negative correlations with mean luminance (LO-2: $r = -0.429$, $p = 0.0142$; and hMT: $r = -0.433$, $p = 0.0134$) and luminance RMS contrast (LO-2: $r = -0.442$, $p = 0.0112$; and hMT+: $r = -0.431$, $p = 0.0138$).

Experiment 2: attention-induced response modulation

We examined the positive response modulation induced by attention to glossiness (glossiness vs. form or glossiness vs. orientation). The neural modulation was also assessed for each of the other two features, form (form vs. glossiness or form vs. orientation) and orientation (orientation vs. glossiness or orientation vs. form).

SPM analysis

Using SPM analysis, we identified nine activation clusters that met the criteria of cluster-level FDR control (Table 3). For the positive response modulation induced by attention to glossiness, we identified a cluster of activation in the ventral part of the occipitotemporal cortex (Fig. 12a). Aside from the visual cortex, we identified two clusters situated in the left inferior frontal gyrus and in the putamen. For modulation induced by attention to form, a cluster was identified in the medial occipital cortex around the calcarine sulcus and the cuneus (Fig. 12b).

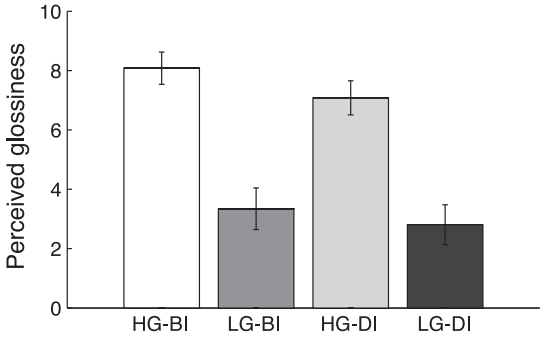

Fig. 9. Perceived glossiness for each of four experimental conditions: high glossiness under bright illumination (HG-BI), low glossiness under bright illumination (LG-BI), high glossiness under dim illumination (HG-DI), and low glossiness under dim illumination (LG-DI). Rating scores indicate perceived level of glossiness with zero indicating no glossiness and 10 indicating glossiness of the standard stimulus. Error bars indicate SEMs.

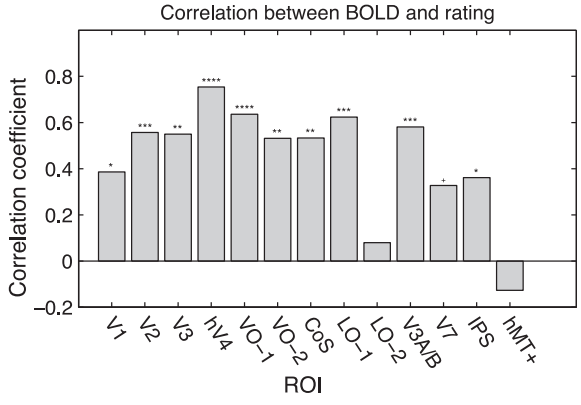

Fig. 10. Correlation between BOLD signal change and perceived glossiness measured in rating experiment. The significance level is indicated by stars and asterisks ($^{+}$: $p < 0.1$ (tendency); *: $p < 0.05$; ***: $p < 0.001$; ****: $p < 0.0001$).

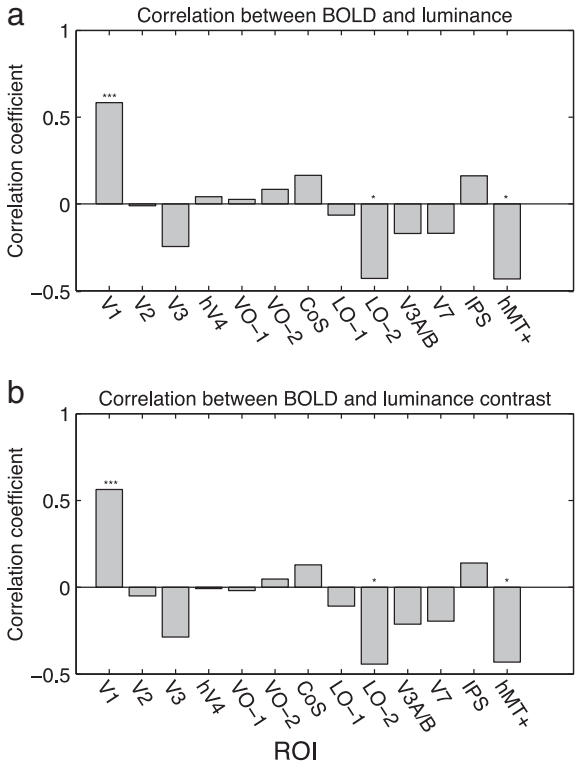

Fig. 11. Correlation between BOLD signal change and (a) mean luminance or (b) RMS luminance contrast. The significance level is indicated by stars (*: $p < 0.05$; ***: $p < 0.001$; and ****: $p < 0.0001$).

Aside from the visual cortex, one cluster was found around the vermis of the cerebellum or the cistern of the great cerebral vein. For the modulation induced by attention to orientation, three clusters (one in the left hemisphere and two in the right hemisphere) were identified in the regions ranging from the IPS to a lateral part of the occipitotemporal cortex. They included the middle temporal gyrus and the caudal part of the IPS (CIP) in both hemispheres and the anterior part of the IPS (AIP) in the right hemisphere (Fig. 12c). The activation observed in these IPS regions seems reasonable, because previous studies reported activation in the same regions, AIP and CIP, for attention to surface orientation (Cant and Goodale, 2007; Shikata et al., 2001). Aside from the visual cortex, the same contrast identified a cluster that situated around the inferior frontal gyrus and the insula.

ROI analysis

The attention-induced response modulation was investigated on an ROI basis. The positive response modulation induced by each of the three features was assessed by the comparisons between the targeting condition and each of the other two conditions (Table 4 and Fig. 13). Owing to the relatively lateralized activation patterns observed in the SPM analysis results, the left and right hemispheres were separately studied for each ROI. The positive modulation induced by attention to glossiness was identified in right hV4, right VO-2, and right V3A/B, which showed significance in the comparison with the orientation condition (right hV4: $p = 0.005$; right VO-2: $p = 0.003$; and V3A/B: $p = 0.030$). We discuss whether such hemispheric laterality in these regions may not be essential but due to some vascular aspects as discussed in Supplementary Analysis 2 and Supplementary Discussion 1. For the positive modulation induced by attention to form, no ROI was identified that showed significance in either comparison. The positive modulation induced by attention to orientation was identified in bilateral hMT+, where both hMT+ showed significance in the comparison with the glossiness condition (left: $p = 0.012$; and right: $p = 0.0012$), and right hMT+ showed significance in the comparison with the form condition ($p = 0.020$).

Behavioral analysis

The behavioral task performance (percent accuracy) of each of the three experimental conditions (glossiness: $M = 98.3$, $SEM = 0.8$; form: $M = 99.1$, $SEM = 0.3$; and orientation: $M = 98.5$, $SEM = 0.5$) was subjected to a one-way repeated-measures ANOVA, where no significant difference ($F_{2,18} = 2.30$, $p = 0.129$) was found. Accordingly, we discuss in Supplementary Discussion 2 that there is unlikely to be a confounding effect of task performance on the results of the ROI analysis in the preceding section (ROI analysis section).

Table 3
Results of SPM conjunction analysis of Experiment 2, averaged across 10 subjects. Clusters of statistically significant contiguous activation were identified (FDR-corrected $p < 0.05$, cluster level).

Region name	Laterality	Peak MNI coordinate			Peak value	Cluster size
		x	y	z	(Z-score)	(# voxels)
(a) Activation related to attention to glossiness						
Occipitotemporal cortex						
Inferior occipital and fusiform gyri	(R)	30	−72	−10	4.96	370
Frontal cortex						
Inferior frontal gyrus	(L)	−48	32	0	4.92	316
Basal ganglia						
Putamen	(L)	−22	10	−2	4.88	155
(b) Activation related to attention to form						
Cerebellum						
Vermis	(LR)	4	−48	2	5.48	232
Occipital cortex						
Calcarine sulcus and cuneus	(L)	−4	−90	8	4.82	282
(c) Activation related to attention to orientation						
Parietal and occipitotemporal cortex						
Intraparietal sulcus (AIP, CIP) and Middle temporal gyrus	(R)	40	−40	46	Inf.	4038
Middle temporal gyrus	(L)	−38	−62	6	6.59	621
Intraparietal sulcus (CIP)	(L)	−12	−68	52	5.24	160
Frontal cortex						

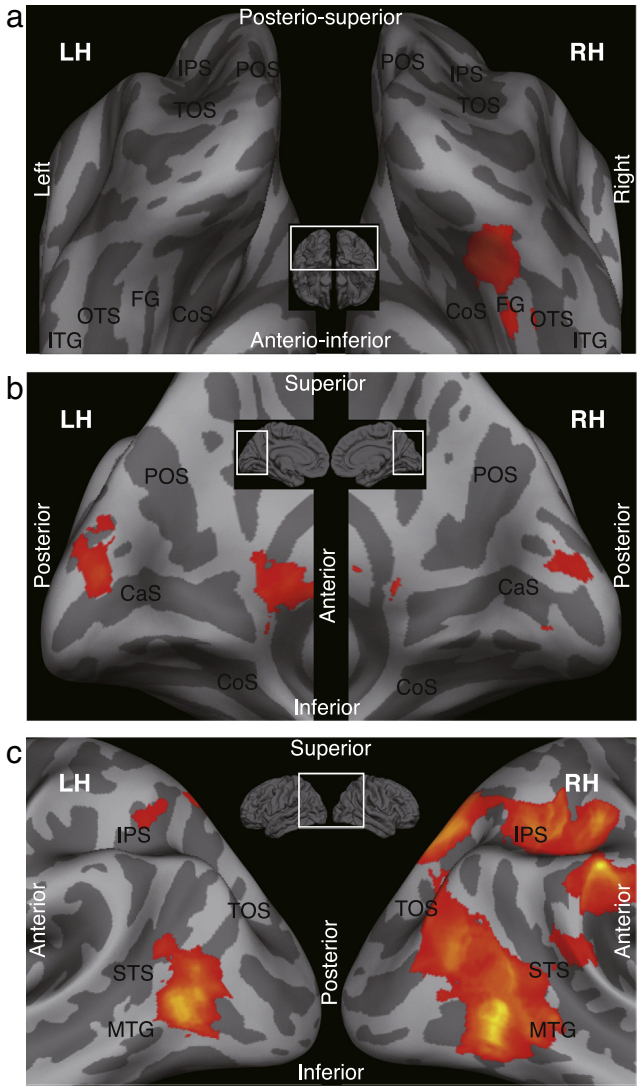

Fig. 12. Results of SPM analysis of Experiment 2, averaged across 10 subjects. Significantly activated clusters identified by SPM conjunction analysis were rendered on fsaverage, an averaged cortical surface provided with FreeSurfer (FDR-corrected $p < 0.05$, cluster level). (a) Glossiness-related contrast comparing glossiness condition with form or orientation condition. (b) Form-related contrast comparing form condition with glossiness or orientation condition. (c) Orientation-related contrast comparing orientation condition with glossiness or form condition. CoS, collateral sulcus; FG, fusiform gyrus; OTS, occipitotemporal sulcus; ITG, inferior temporal gyrus; POS, parieto-occipital sulcus; CaS, calcarine sulcus; IPS, intraparietal sulcus; TOS, transverse occipital sulcus; MTG, middle temporal gyrus; STS, superior temporal sulcus; LH, left hemisphere; RH, right hemisphere.

Table 4
Results of ROI analysis of Experiment 2, averaged across eight subjects. P-values for each of the three pairwise comparisons were computed for each ROI (Bonferroni corrected). G: glossiness; F: form; O: orientation.

ROI	G vs. F p-value	G vs. O p-value	F vs. O p-value	ROI	G vs. F p-value	G vs. O p-value	F vs. O p-value
lV1	0.950	0.449	0.078^{+} (F > O)	rV1	0.816	0.542	0.072^{+} (F > O)
lV2	0.831	0.724	0.246	rV2	1.000	0.176	0.065^{+} (F > O)
lV3	1.000	1.000	1.000	rV3	1.000	0.055^{+} (G > O)	0.085^{+} (F > O)
lhV4	1.000	1.000	1.000	rhV4	0.379	0.005** (G > O)	0.929
lVO1	1.000	1.000	1.000	rVO1	1.000	0.241	1.000
lVO2	1.000	1.000	1.000	rVO2	1.000	0.003** (G > O)	0.907
lCoS	1.000	1.000	1.000	rCoS	1.000	1.000	1.000
lLO1	1.000	0.433	0.316	rLO1	1.000	0.492	0.486
lLO2	0.904	1.000	1.000	rLO2	1.000	0.644	1.000
lV3A/B	1.000	0.083^{+} (G > O)	0.220	rV3A/B	1.000	0.030* (G > O)	0.587
lV7	0.960	0.993	0.277	rV7	1.000	1.000	1.000
lIPS	1.000	1.000	1.000	rIPS	1.000	0.512	0.388
lhMT+	0.175	0.012* (G < O)	1.000	rhMT+	0.301	0.001** (G < O)	0.020* (F < O)

$^{+}$ $p < 0.1$ (tendency).
* $p < 0.05$.
** $p < 0.01$.

Discussion

Visual cortical regions involved in the processing of glossiness

In this study we performed two fMRI experiments with different paradigms to reliably and comprehensively investigate which regions in the visual cortex are involved in the processing of glossiness. Experiment 1 examined stimulus-induced neural responses to high compared with low glossiness while the visual system was actively engaged in glossiness discrimination, which identified V2, V3, hV4, VO-1, VO-2, CoS, LO-1, and V3A/B as the possible regions that responded to high compared with low glossiness regardless of the differences in illumination level (Experiment 1: stimulus-induced neural response section and Table 2). Experiment 2 examined neural modulation induced by attention to glossiness, which identified right hV4, right VO-2, and right V3A/B as regions that elicited higher positive modulation to attention to glossiness than to either form or orientation (Experiment 2: attention-induced response modulation section and Table 4).

It appears certain that the regions hV4, VO-2, and V3A/B play important roles in glossiness processing, because these regions were commonly identified by the two experiments. On the other hand, we consider that the regions identified only in Experiment 1, i.e. V2, V3, VO-1, CoS, and LO-1, have some roles in glossiness processing, such as extracting visual features used for glossiness estimation, which may not be specialized for glossiness processing, or higher processing induced by glossiness processing. Such possibilities will be discussed in subsequent sections. One might suppose that these regions were activated by visual features coincidently co-varied with glossiness but not those directly associated with glossiness, but this presumption may not apply because involvement of these regions in glossiness processing conforms to previous monkey studies, which will also be discussed later in Relationship to human lesion and monkey studies section.

When viewing the results of the present study with respect to the ventral and dorsal visual pathways (Goodale, 1992; Milner and Goodale, 2006; Ungerleider and Mishkin, 1982), the involvement of both the ventral pathway, including hV4 and VO-2, and the dorsal pathway, including V3A/B, was suggested. The reason why the processing of glossiness requires the involvement of such broad regions in multiple visual pathways might be due to the nature of glossiness estimation when viewed from a computational perspective. As mentioned in the introduction, the estimation of glossiness from a retinal image is a computationally hard problem, where the image intensity depends not only on the surface reflectance properties but also on the light source intensity and the geometrical relationships between the light sources, the surface orientation, and the viewpoint. To solve this hard problem, humans seem to use multiple glossiness cues including color relationship between the highlight and the surrounding areas (Nishida et al., 2008, 2011) and the highlight orientation consistent with the shading of the surface (Anderson and Kim, 2009; Kim et al., 2011; Marlow et al., 2011). The results of the present study imply that the processing of such glossiness cues might be distributed in both dorsal and ventral visual pathways. In the following sections, we further discuss from a functional aspect

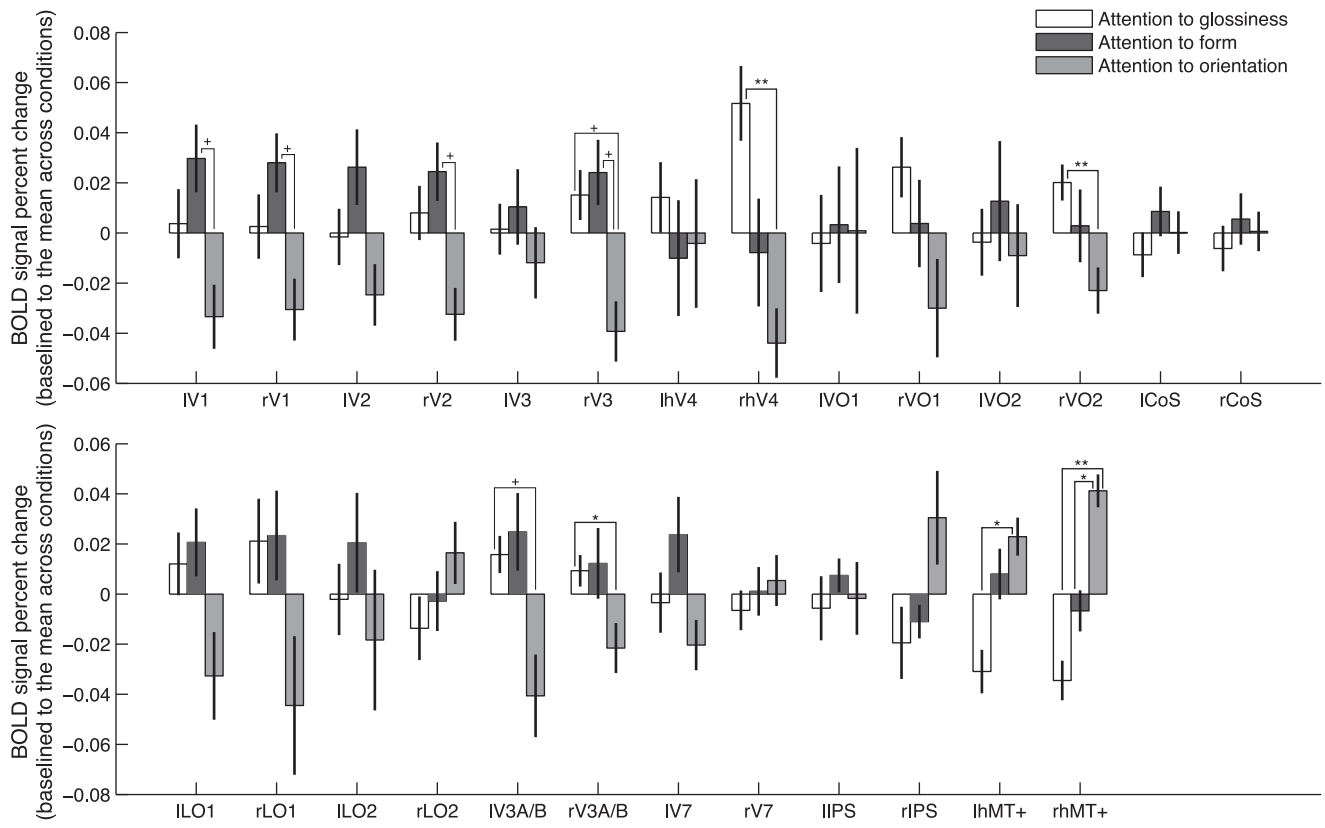

Fig. 13. Results of ROI analysis of Experiment 2. For each ROI, BOLD signal percent change was baselined to mean across conditions and averaged across eight subjects. Statistical significance for the difference of the mean activation levels between the experimental conditions was highlighted by pluses and asterisks ($^{+}$: $p < 0.1$ (tendency); *: $p < 0.05$; and ***: $p < 0.001$).

how each of the identified regions might play a role in glossiness estimation.

Relationship between the processing of glossiness and surface properties in the ventral visual cortex

In the ventral visual pathway, hV4 and VO-2 were commonly identified by the stimulus-based and attention-based paradigms used in Experiments 1 and 2, respectively (Experiment 1: stimulus-induced neural response and Experiment 2: attention-induced response modulation sections). Here, we discuss the implications of this result in relation to previous findings that suggest the functions of the ventral visual pathway, especially from the perspective of the processing of surface properties.

Visual area hV4 is known to play significant roles in visual perception. Particularly, its previously reported functions include the processing of texture segregation (Thielscher et al., 2008), object surface perception (Bouvier et al., 2008), and color constancy (Barbur and Spang, 2008; Bartels and Zeki, 2000; Clarke et al., 1998; Kennard et al., 1995). Here, we speculate that hV4 might be estimating the surface properties of objects, which, in principle, requires the following two computational processes: (1) the segregation of object surface regions in a retinal image; and (2) the dissociation of reflectance properties and illumination conditions in the object surface regions. The former process may be relevant to texture segregation and surface perception. The latter may be relevant to color constancy, which requires the estimation of surface spectral reflectance invariant to illumination color. In this view, glossiness processing can be similarly defined as the estimation of surface directional reflectance properties invariant to illumination conditions, and thus may also be relevant to the latter process. Therefore, we hypothesize that one of the important functional roles of hV4 is to identify object surfaces and describe their reflectance properties, including surface glossiness, by dissociating the effect of illumination, which may reasonably explain the results of our experiments and the previously reported studies on the functions of hV4.

VO-2, which is another visual area we identified as a region involved in glossiness processing, resides in the ventral visual cortex near CoS (Brewer et al., 2005; Larsson and Heeger, 2006; Liu and Wandell, 2005). Unfortunately, it is difficult to infer the role of VO-2 in glossiness processing because the functions of VO-2 are not well understood. The only study that examined its visual processing characteristics was Brewer et al. (2005), which reported that VO-2 responded preferentially to objects compared with faces. In the neighboring regions, it has been reported that VO-1 is involved in second-order texture perception (Larsson et al., 2006) and CoS in the processing of material (Cant and Goodale, 2011; Hiramatsu et al., 2011), where both regions showed significant responses to high vs. low glossiness in our Experiment 1 (Experiment 1: stimulus-induced neural response section and Table 2). Additionally, a psychophysical study has reported that the perceived glossiness might be used for recognizing materials (Ged et al., 2010). Thus, regions including VO-2, and possibly the neighboring areas VO-1 and CoS, might be playing a role in processing glossiness in relation to their role in processing surface textures and materials. Further investigation is required to clarify the role of these regions in the processing of glossiness.

In these regions, the BOLD signal change tended to show a larger response to the attention to form compared with that to orientation (although no significant effect was found). Thus, we speculate that such a response profile might be elicited by the involvement of the regions identified in the ventral cortex, not only in the processing of glossiness, but also partially in processing an object, particularly related to its form. This assumption somewhat conforms to previous fMRI studies that suggest the involvement of the ventral visual pathway in object recognition (Grill-Spector et al., 2004; Ishai et al., 2000; Kanwisher et al., 1997). In this view, the partial involvement of LO-1 in the lateral occipital region in the glossiness processing shown only

by Experiment 1 (Experiment 1: stimulus-induced neural response section and Table 2) could also be interpreted as due to object processing induced by glossiness cues rather than glossiness processing itself, which seems to be consistent with previous studies that have reported the lateral occipital region as playing a significant role in the perception of objects from their contour (Kourtzi and Kanwisher, 2000; Malach et al., 1995). Further investigation is needed in future work to clarify whether the lateral occipital areas are involved in the processing of glossiness.

Relationship between the processing of glossiness and object 3D shape in the dorsal visual cortex

In the dorsal visual pathway, V3A/B was commonly identified by the stimulus-based and attention-based paradigms used in Experiments 1 and 2, respectively (Experiment 1: stimulus-induced neural response and Experiment 2: attention-induced response modulation sections). As previous fMRI studies on V3A/B have reported the involvement of these regions in the processing of shape from shading (Gerardin et al., 2010) and object shape estimation (Preston et al., 2009), we speculate that a possible functional role of V3A/B in glossiness processing might be the estimation of glossiness that needs to take an object's 3D form into account for its computation. This seems likely because psychophysical studies have reported the effect of object shape on glossiness perception (Anderson and Kim, 2009; Kim et al., 2011; Marlow et al., 2011), where perceived glossiness decreases when specular highlights are inconsistent with object shape estimated from shading.

One might interpret the results as reflecting the involvement of V3A/B in the processing of a 3D shape based on glossiness cues, which is consistent with a psychophysical study that reported the effect of glossiness cues, especially the specular reflection on object surface, on the estimation of object shape (Blake and Bülthoff, 1990; Blake and Bülthoff, 1991; Fleming et al., 2004; but see Nefs et al., 2006). This idea somewhat conforms with the results of Experiment 2, where no significance was found in the comparison between attention to glossiness vs. form conditions, whereas the BOLD signal change tended to show a larger response to attention to form compared with that to orientation (although no significant effect was found). Thus, we speculate that V3A/B might be involved not only in the estimation of glossiness in relation to an object's 3D shape, but that it could also be involved in the processing of form using glossiness cues. Further investigations are needed in future work to clarify how human V3A/B is involved in the estimation of glossiness in relation to that of an object's 3D shape.

V3 showed a significant effect induced by the bottom-up processing of glossiness in Experiment 1 (Experiment 1: stimulus-induced neural response section and Table 2) and tended to show modulation induced by attention to glossiness in the second ROI analysis in Experiment 2 (Experiment 2: attention-induced response modulation section and Table 4). Since V3 may play a greater role in dorsal than in ventral visual processing (see Lyon and Connolly, 2012 for a review), we speculate that the processing of glossiness in V3 could be contributing to glossiness processing in the dorsal visual stream, as in V3A/B, where the estimation of glossiness regarding 3D object shape might take place.

Relationship between glossiness processing and the computation of low-level visual features in the early visual cortex

In the early visual cortex, where the processing of elementary visual features is known to take place, V2 was identified as possible glossiness processing regions by Experiment 1 but not by Experiment 2 (Experiment 1: stimulus-induced neural response and Experiment 2: attention-induced response modulation sections), which suggests that V2 might be related to glossiness processing but is less likely to play a central role. Here, we discuss whether the computations of low-level visual features in the early visual cortex, especially local luminance contrast and skewness of the luminance histogram, could be related to the estimation of glossiness.

Previous human neuroimaging studies on luminance contrast reported neural responses in V2 (Boynton et al., 1999; Gardner et al., 2005). Conversely, psychophysical studies have reported that luminance contrast locally distributed along the object surface, which is often derived by specular highlights, is an important cue for estimating glossiness (e.g., Ferwerda et al., 2001; Hunter and Harold, 1987; Marlow and Anderson, 2013; Marlow et al., 2012). Thus, although the effect of luminance contrast was controlled globally by illumination factors in Experiment 1, we speculate that local luminance contrast as a cue to glossiness is detected in the early visual cortex so that later in the higher visual areas such as VO-2 and V3A/B, it is judged whether the detected luminance contrast is caused by specular reflection (i.e., gloss), texture, or shading.

Another possible role of V2 in glossiness estimation could be the computation of skewness of the luminance histogram, because a skewness detection model proposed by Motoyoshi et al. (2007) requires contrast sign responsive cells, which have been reported to reside in V1 or V2 (Kagan et al., 2002; Shipp and Zeki, 2002). The skewness, which might be detected in V2, could then be used to estimate glossiness in such subsequent areas as hV4 as mentioned above.

On the other hand, unlike V2, V1 did not show a significant neural response to high vs. low glossiness but did show one to illumination difference (Experiment 1: stimulus-induced neural response section and Table 2). Thus although it showed significant neural correlates to perceived level of glossiness, the involvement of V1 in glossiness processing is difficult to assert from our current results.

Relationship to human lesion and monkey studies

The identified ROIs, except for V3A/B, were located in the ventral visual pathway ranging from the early visual to higher ventral visual cortices (Experiment 1: stimulus-induced neural response and Experiment 2: attention-induced response modulation sections). These identified areas in the ventral visual pathway seem consistent with a previous monkey fMRI study that identified selective neural responses to specular surfaces in the ventral visual pathway including V1, V2, V3, V4, and the posterior IT cortex, but not the dorsal visual pathway including MT+ and IPS (Okazawa et al., 2012). A similar correspondence was found for the dorsal visual pathway in our results, where hMT+, V7 and IPS did not show a significant main effect of glossiness. The only region that showed inconsistency between our human and previous monkey studies was V3A/B in the dorsal visual cortex. Despite the involvement of V3A/B in human dorsal visual cortex suggested by our current results, the previous monkey study found no selective neural responses to glossiness in the dorsal visual cortex. This inconsistency implies that the dorsal visual pathway is involved in glossiness processing in humans, but not in monkeys, which conforms to the behavioral results of Kentridge et al. (2012), where a visual agnosic subject, M.S., with a lesioned ventral visual cortex and an intact dorsal visual cortex, was reported to be able to discriminate glossiness at above chance levels. As the differences between humans and monkeys in the functions of V3A have also been reported (Tootell et al., 1997; Vanduffel et al., 2001; for review, see Orban et al., 2003), we hypothesize that the involvement of V3A/B in glossiness processing might be specific to the human visual system.

Regarding the neural representation of glossiness, we assumed in our analysis that the cortical regions involved in glossiness would elicit higher neural activation for high compared with low glossiness stimuli. We consider this assumption to be reasonable based on the results of the previous monkey studies on glossiness. Nishio et al. (2012) reported in their single-unit recording study that although they found a variety of gloss-selective neurons whose neuronal selectivity to the level of glossiness varied from high (glossy) to low (matte), as a population the neurons preferred glossy to matte surfaces. Okazawa et al. (2012) found, in

their fMRI study, broad regions in the ventral visual pathway that were activated more in the specular compared with the matte condition, but none that responded more strongly in the matte than the specular condition. Similarly, in the present fMRI study on humans, the result of the ROI analysis of Experiment 1 identified multiple ROIs that showed significant activation to the high vs. low glossiness conditions, but none that showed significance for the low vs. high glossiness conditions. Thus, the neural representation of glossiness in humans might be similar to that reported in the monkey studies as described above, where the population responses in the human cortical regions involved in glossiness could reflect the level of glossiness.

Conclusions

We reported the first human neuroimaging study to investigate the neural substrates of glossiness perception. Experiment 1 identified stimulus-induced response to glossiness in V2, V3, hV4, VO-1, VO-2, CoS, LO-1, and V3A/B, which also showed significant correlation with perceived glossiness. Experiment 2 found response modulation induced by selective attention to glossiness in right hV4, right VO-2, and right V3A/B. Since these three areas (i.e., hV4, VO-2, and V3A/B) are identified commonly in the two experiments with different paradigms, we conclude that these areas are involved in glossiness processing with high certainty. The involvement of V3A/B in glossiness processing might be human-specific because a previous monkey study did not find any dorsal areas that are involved in the processing of surface gloss. In terms of the roles of the three areas identified in the present study, we speculate that, based on our results together with previous psychophysical and neuroimaging studies, hV4 is involved in estimation of surface reflectance properties invariant to illumination conditions, VO-2 in glossiness processing associated with surface textures and materials, and V3A/B in glossiness computation related to the object's 3D shape. In summary, the present study provides evidence indicating the coexisting contributions of both the ventral and dorsal visual pathways in the processing of glossiness in humans, but it remains an open question whether and how these areas constitute a cortical network for the estimation of surface glossiness.

Acknowledgments

We thank Yasuhiro Shimada, Ichiro Fujimoto, and Hironori Nishimoto who prepared the experiments and collected imaging data, Takanori Kochiyama for his support in statistical analysis, Naho Orita for her significant help with data processing and analysis, and Norberto Eiji Nawa, Akiko Callan, Yurie Nishino, and Hiroshi Ashida for their helpful suggestion and comments.

Conflict of interest

None.

Appendix A. Supplementary data

Supplementary data to this article can be found online at http://dx.doi.org/10.1016/j.neuroimage.2014.05.001.

References

Adelson, E.H., 2001. On seeing stuff: the perception of materials by humans and machines. Proc SPIE.
Amano, K., Wandell, B.A., Dumoulin, S.O., 2009. Visual field maps, population receptive field sizes, and visual field coverage in the human MT+ complex. J. Neurophysiol. 102 (5), 2704–2718.
Anderson, B.L., Kim, J., 2009. Image statistics do not explain the perception of gloss and lightness. J. Vis. 9 (11), 1–17 (10).
Avidan, G., Harel, M., Hendler, T., Ben-Bashat, D., Zohary, E., Malach, R., 2002. Contrast sensitivity in human visual areas and its relationship to object recognition. J. Neurophysiol. 87 (6), 3102–3116.
Barbur, J.L., Spang, K., 2008. Colour constancy and conscious perception of changes of illuminant. Neuropsychologia 46, 853–863.
Bartels, A., Zeki, S., 2000. The architecture of the colour centre in the human visual brain: new results and a review. Eur. J. Neurosci. 12 (1), 172–193.
Beck, J., Prazdny, S., 1981. Highlights and the perception of glossiness. Percept. Psychophys. 30 (4), 407–410.
Bertero, M., Poggio, T.A., Torre, V., 1988. Ill-posed problems in early vision. Proc IEEE, pp. 869–889.
Berzhanskaya, J., Swaminathan, G., Beck, J., Mingolla, E., 2005. Remote effects of highlights on gloss perception. Perception 34 (5), 565–575.
Blake, A., Bülthoff, H., 1990. Does the brain know the physics of specular reflection? Nature 343 (6254), 165–168.
Blake, A., Bülthoff, H., 1991. Shape from specularities: computation and psychophysics. Philos. Trans. R. Soc. Lond. B Biol. Sci. 331, 237–252.
Bouvier, S.E., Cardinal, K.S., Engel, S.A., 2008. Activity in visual area V4 correlates with surface perception. J. Vis. 8 (28), 1–9.
Boynton, G.M., Engel, S.A., Glover, G.H., Heeger, D.J., 1996. Linear systems analysis of functional magnetic resonance imaging in human V1. J. Neurosci. 16 (13), 4207–4221.
Boynton, G.M., Demb, J.B., Glover, G.H., Heeger, D.J., 1999. Neuronal basis of contrast discrimination. Vis. Res. 39 (2), 257–269.
Brewer, A.A., Liu, J., Wade, A.R., Wandell, B.A., 2005. Visual field maps and stimulus selectivity in human ventral occipital cortex. Nat. Neurosci. 8 (8), 1102–1109.
Cant, J.S., Goodale, M.A., 2007. Attention to form or surface properties modulates different regions of human occipitotemporal cortex. Cereb. Cortex 17 (3), 713.
Cant, J.S., Goodale, M.A., 2011. Scratching beneath the surface: new insights into the functional properties of the lateral occipital area and parahippocampal place area. J. Neurosci. 31 (22), 8248–8258.
Cant, J.S., Arnott, S.R., Goodale, M.A., 2009. fMR-adaptation reveals separate processing regions for the perception of form and texture in the human ventral stream. Exp. Brain Res. 192 (3), 391–405.
Clarke, S., Walsh, V., Schoppig, A., Assal, G., Cowey, A., 1998. Colour constancy impairments in patients with lesions of the prestriate cortex. Exp. Brain Res. 123, 154–158.
Corbetta, M., Miezin, F., Dobmeyer, S., Shulman, G., Petersen, S., 1990. Attentional modulation of neural processing of shape, color, and velocity in humans. Science 248, 1556.
DeYoe, E.A., Carman, G.J., Bandettini, P., Glickman, S., Wieser, J., Cox, R., Miller, D., Neitz, J., 1996. Mapping striate and extrastriate visual areas in human cerebral cortex. Proc. Natl. Acad. Sci. U. S. A. 93 (6), 2382–2386.
Doerschner, K., Fleming, R.W., Yilmaz, O., Schrater, P.R., Hartung, B., Kersten, D., 2011. Visual motion and the perception of surface material. Curr. Biol. 21, 2010–2016.
Dror, R.O., Adelson, E.H., Willsky, A.S., 2001. Surface reflectance estimation and natural illumination statistics. Proc IEEE Workshop on Statistical and Computational Theories of Vision.
Engel, S.A., Rumelhart, D.E., Wandell, B.A., Lee, A.T., Glover, G.H., Chichilnisky, E.J., Shadlen, M.N., 1994. fMRI of human visual cortex. Nature 369 (6481), 525.
Ferwerda, J.A., Pellacini, F., Greenberg, D.P., 2001. A psychophysically-based model of surface gloss perception. Proc SPIE Human Vision and Electronic Imaging VI, pp. 291–301.
Fleming, R.W., Dror, R.O., Adelson, E.H., 2003. Real-world illumination and the perception of surface reflectance properties. J. Vis. 3 (5), 347–368.
Fleming, R.W., Torralba, A., Adelson, E.H., 2004. Specular reflections and the perception of shape. J. Vis. 4, 798–820.
Gangestad, S.W., Scheyd, G.J., 2005. The evolution of human physical attractiveness. Annu. Rev. Anthropol. 34 (1), 523–548.
Gardner, J.L., Sun, P., Waggoner, R.A., Ueno, K., Tanaka, K., Cheng, K., 2005. Contrast adaptation and representation in human early visual cortex. Neuron 47 (4), 607–620.
Ged, G., Obein, G., Silvestri, Z., Le Rohellec, J., Vienot, F., 2010. Recognizing real materials from their glossy appearance. J. Vis. 10 (9), 1–17 (18).
Georgieva, S.S., Todd, J.T., Peeters, R., Orban, G.A., 2008. The extraction of 3D shape from texture and shading in the human brain. Cereb. Cortex 18 (10), 2416–2438.
Gerardin, P., Kourtzi, Z., Mamassian, P., 2010. Prior knowledge of illumination for 3D perception in the human brain. Proc. Natl. Acad. Sci. U. S. A. 107, 16309–16314.
Goodale, M.A., 1992. Separate visual pathways for perception and action. Trends Neurosci. 15, 20–25.
Grill-Spector, K., Malach, R., 2004. The human visual cortex. Annu. Rev. Neurosci. 27, 649–677.
Grill-Spector, K., Knouf, N., Kanwisher, N., 2004. The fusiform face area subserves face perception, not generic within-category identification. Nat. Neurosci. 7, 555–562.
Hall, S.D., Holliday, I.E., Hillebrand, A., Furlong, P.L., Singh, K.D., Barnes, G.R., 2005. Distinct contrast response functions in striate and extra-striate regions of visual cortex revealed with magnetoencephalography (MEG). Clin. Neurophysiol. 116 (7), 1716–1722.
Hartung, B., Kersten, D., 2002. Distinguishing shiny from matte. J. Vis. 2 (7) (551-551).
Heeger, D.J., Huk, A.C., Geisler, W.S., Albrecht, D.G., 2000. Spikes versus BOLD: what does neuroimaging tell us about neuronal activity? Nat. Neurosci. 3 (7), 631–633.
Hering, E., 1964. Outlines of a Theory of the Light Sense. In: Hurvich, L.M., Jameson, D. (Eds.), Harvard University Press, Cambridge (MA) (344 p.).
Hiramatsu, C., Goda, N., Komatsu, H., 2011. Transformation from image-based to perceptual representation of materials along the human ventral visual pathway. Neuroimage 57 (2), 482–494.
Horiguchi, H., Nakadomari, S., Misaki, M., Wandell, B.A., 2009. Two temporal channels in human V1 identified using fMRI. Neuroimage 47 (1), 273–280.
Horn, B.K.P., 1977. Understanding image intensities. Artif. Intell. 8 (2), 201–231.
Horn, B.K.P., Sjoberg, R.W., 1979. Calculating the reflectance map. Appl. Opt. 18 (11), 1770–1779.
Huk, A.C., Dougherty, R.F., Heeger, D.J., 2002. Retinotopy and functional subdivision of human areas MT and MST. J. Neurosci. 22 (16), 7195–7205.
Hunter, R.S., Harold, R.W., 1987. The Measurement of Appearance. John Wiley & Sons, New York (NY) (411 p).

Hurlbert, A., Cumming, B., Parker, A., 1991a. Constraints of specularity motion on glossiness and shape perception. Paper presented at ECVP 1991 (1-1).
Hurlbert, A., Cumming, B., Parker, A., 1991b. Recognition and perceptual use of specular reflections. Invest. Ophthalmol. Vis. Sci. Suppl. 32 (4), 105.
Ishai, A., Ungerleider, L.G., Martin, A., Haxby, J.V., 2000. The representation of objects in the human occipital and temporal cortex. J. Cogn. Neurosci. 12 (Suppl. 2), 35–51.
Kagan, I., Gur, M., Snodderly, D.M., 2002. Spatial organization of receptive fields of V1 neurons of alert monkeys: comparison with responses to gratings. J. Neurophysiol. 88, 2557–2574.
Kanwisher, N., McDermott, J., Chun, M.M., 1997. The fusiform face area: a module in human extrastriate cortex specialized for face perception. J. Neurosci. 17, 4302–4311.
Kennard, C., Lawden, M., Morland, A.B., Ruddock, K.H., 1995. Colour identification and colour constancy are impaired in a patient with incomplete achromatopsia associated with prestriate cortical lesions. Proc. Biol. Sci. 22;260 (1358), 169–175.
Kentridge, R.W., Thomson, R., Heywood, C.A., 2012. Glossiness perception can be mediated independently of cortical processing of colour or texture. Cortex 48 (9), 1244–1246.
Kim, J., Marlow, P., Anderson, B.L., 2011. The perception of gloss depends on highlight congruence with surface shading. J. Vis. 11 (9), 1–19 (4).
Kourtzi, Z., Kanwisher, N., 2000. Cortical regions involved in perceiving object shape. J. Neurosci. 20 (9), 3310–3318.
Larsson, J., Heeger, D.J., 2006. Two retinotopic visual areas in human lateral occipital cortex. J. Neurosci. 26 (51), 13128–13142.
Larsson, J., Landy, M.S., Heeger, D.J., 2006. Orientation-selective adaptation to first- and second-order patterns in human visual cortex. J. Neurophysiol. 95, 862–881.
Liu, J., Wandell, B.A., 2005. Specializations for chromatic and temporal signals in human visual cortex. J. Neurosci. 25 (13), 3459–3468.
Liu, T., Slotnick, S.D., Serences, J.T., Yantis, S., 2003. Cortical mechanisms of feature-based attentional control. Cereb. Cortex 13, 1334–1343.
Logothetis, N.K., Pauls, J., Augath, M., Trinath, T., Oeltermann, A., 2001. Neurophysiological investigation of the basis of the fMRI signal. Nature 412 (6843), 150–157.
Lyon, D.C., Connolly, J.D., 2012. The case for primate V3. Proc. R. Soc. B 279, 626–633.
Malach, R., Reppas, J.B., Benson, R.R., Kwong, K.K., Jiang, H., Kennedy, W.A., Ledden, P.J., Brady, T.J., Rosen, B.R., Tootell, R.B., 1995. Object-related activity revealed by functional magnetic resonance imaging in human occipital cortex. Proc. Natl. Acad. Sci. U. S. A. 92 (18), 8135–8139.
Marlow, P.J., Anderson, B.L., 2013. Generative constraints on image cues for perceived gloss. J. Vis. 13 (14), 1–23 (2).
Marlow, P., Kim, J., Anderson, B.L., 2011. The role of brightness and orientation congruence in the perception of surface gloss. J. Vis. 11 (9), 1–12 (16).
Marlow, P.J., Kim, J., Anderson, B.L., 2012. The perception and misperception of specular surface reflectance. Curr. Biol. 22 (20), 1909–1913.
Milner, A.D., Goodale, M.A., 2006. The Visual Brain in Action. Oxford University Press, USA, New York (NY) (297 p.).
Mizrach, A., Lu, R., Rubino, M., 2008. Gloss evaluation of curved-surface fruits and vegetables. Food Bioprocess Technol. 2 (3), 300–307.
Motoyoshi, I., Sy, Nishida, Sharan, L., Adelson, E.H., 2007. Image statistics and the perception of surface qualities. Nature 447 (7141), 206–209.
Murray, S.O., Wojciulik, E., 2004. Attention increases neural selectivity in the human lateral occipital complex. Nat. Neurosci. 7, 70–74.
Nefs, H.T., Koenderink, J.J., Kappers, A.M.L., 2006. Shape-from-shading for matte and glossy objects. Acta Psychol. (Amst). 121, 297–316.
Nicodemus, F.E., Richmond, J.C., Hsia, J.J., Ginsberg, I.W., Limperis, T., 1977. Geometrical Considerations and Nomenclature for Reflectance. U.S. Department of Commerce. National Bureau of Standards, Washington, D.C. (DC).
Nishida, S., Shinya, M., 1998. Use of image-based information in judgments of surface-reflectance properties. J. Opt. Soc. Am. A Opt. Image Sci. Vis. 15, 2951–2965.
Nishida, S., Motoyoshi, I., Nakano, L., Li, Y., Sharan, L., Adelson, E., 2008. Do colored highlights look like highlights? J. Vis. 8 (6) (339-339).
Nishida, S., Motoyoshi, I., Maruya, K., 2011. Luminance-color interactions in surface gloss perception. J. Vis. 11 (11) (397-397).
Nishio, A., Goda, N., Komatsu, H., 2012. Neural selectivity and representation of gloss in the monkey inferior temporal cortex. J. Neurosci. 32, 10780–10793.
Obein, G., Knoblauch, K., Viénot, F., 2004. Difference scaling of gloss: nonlinearity, binocularity, and constancy. J. Vis. 4 (9), 711–720.
Okazawa, G., Goda, N., Komatsu, H., 2012. Selective responses to specular surfaces in the macaque visual cortex revealed by fMRI. NeuroImage 63, 1321–1333.
Olman, C.A., Ugurbil, K., Schrater, P., Kersten, D., 2004. BOLD fMRI and psychophysical measurements of contrast response to broadband images. Vis. Res. 44 (7), 669–683.
Orban, G.A., Fize, D., Peuskens, H., Denys, K., Nelissen, K., Sunaert, S., Todd, J., Vanduffel, W., 2003. Similarities and differences in motion processing between the human and macaque brain: evidence from fMRI. Neuropsychologia 41, 1757–1768.
Pellacini, F., Ferwerda, J., GreenBerg, D.P., 2000. Toward a psychophysically-based light reflection model for image synthesis. Proceedings of the 27th Annual Conference on Computer Graphics and Interactive Techniques (SIGGRAPH'00).
Phong, B.T., 1975. Illumination for computer generated pictures. Commun. ACM 18 (6), 311–317.
Pont, S.C., te Pas, S.F., 2006. Material-illumination ambiguities and the perception of solid objects. Perception 35 (10), 1331–1350.
Preston, T.J., Kourtzi, Z., Welchman, A.E., 2009. Adaptive estimation of three-dimensional structure in the human brain. J. Neurosci. 29 (6), 1688–1698.
Sakano, Y., Ando, H., 2010. Effects of head motion and stereo viewing on perceived glossiness. J. Vis. 10 (9), 1–14 (15).
Shikata, E., Hamzei, F., Glauche, V., Knab, R., Dettmers, C., Weiller, C., Büchel, C., 2001. Surface orientation discrimination activates caudal and anterior intraparietal sulcus in humans: an event-related fMRI study. J. Neurophysiol. 85 (3), 1309–1314.
Shipp, S., Zeki, S., 2002. The functional organization of area V2, I: specialization across stripes and layers. Vis. Neurosci. 19, 187–210.
Smith, A.T., Greenlee, M.W., Singh, K.D., Kraemer, F.M., Hennig, J., 1998. The processing of first- and second-order motion in human visual cortex assessed by functional magnetic resonance imaging (fMRI). J. Neurosci. 18 (10), 3816–3830.
Swisher, J.D., Halko, M.A., Merabet, L.B., McMains, S.A., Somers, D.C., 2007. Visual topography of human intraparietal sulcus. J. Neurosci. 27 (20), 5326–5337.
Thielscher, A., Kölle, M., Neumann, H., Spitzer, M., Grön, G., 2008. Texture segmentation in human perception: a combined modeling and fMRI study. Neurosci 151, 730–736.
Tootell, R.B., Reppas, J.B., Kwong, K.K., 1995. Functional analysis of human MT and related visual cortical areas using magnetic resonance imaging. J. Neurosci. 15 (4), 3215–3230.
Tootell, R.B., Mendola, J.D., Hadjikhani, N.K., Ledden, P.J., Liu, A.K., Reppas, J.B., Sereno, M.I., Dale, A.M., 1997. Functional analysis of V3A and related areas in human visual cortex. J. Neurosci. 17 (18), 7060–7078.
Ungerleider, L.G., Mishkin, M., 1982. Two cortical visual systems. In: Ingle, D., Goodale, M., Mansfield, R. (Eds.), Analysis of Visual Behavior. The MIT Press, Massachusetts (MA), pp. 549–586.
Vanduffel, W., Fize, D., Mandeville, J.B., Nelissen, K., Van Hecke, P., Rosen, B.R., Tootell, R.B., Orban, G.A., 2001. Visual motion processing investigated using contrast agent-enhanced fMRI in awake behaving monkeys. Neuron 32, 565–577.
Vladusich, T., Lucassen, M.P., Cornelissen, F.W., 2006. Do cortical neurons process luminance or contrast to encode surface properties? J. Neurophysiol. 95 (4), 2638–2649.
von Helmholtz, H., 1910. Treatise on physiological optics. Dover Phoenix Editions. Volume II. Dover Publications, Mineola (NY) (496 p).
Wada, Y., Arce-Lopera, C., Masuda, T., Kimura, A., Dan, I., S-i, Goto, Tsuzuki, D., Okajima, K., 2010. Influence of luminance distribution on the appetizingly fresh appearance of cabbage. Appetite 54 (2), 363–368.
Wandell, B.A., Dumoulin, S.O., Brewer, A.A., 2007. Visual field maps in human cortex. Neuron 56 (2), 366–383.
Warnking, J., Dojat, M., Guérin-Dugué, A., Delon-Martin, C., Olympieff, S., Richard, N., Chéhikian, A., Segebarth, C., 2002. fMRI retinotopic mapping: step by step. Neuroimage 17 (4), 1665–1683.
Watson, J.D., Myers, R., Frackowiak, R.S., Hajnal, J.V., Woods, R.P., Mazziotta, J.C., Shipp, S., Zeki, S., 1993. Area V5 of the human brain: evidence from a combined study using positron emission tomography and magnetic resonance imaging. Cereb. Cortex 3 (2), 79–94.
Wendt, G., Faul, F., Mausfeld, R., 2008. Highlight disparity contributes to the authenticity and strength of perceived glossiness. J. Vis. 8 (1), 1–10 (14).
Wendt, G., Faul, F., Ekroll, V., Mausfeld, R., 2010. Disparity, motion, and color information improve gloss constancy performance. J. Vis. 10 (9), 1–17 (7).
Zeki, S., Watson, J.D., Lueck, C.J., Friston, K.J., Kennard, C., Frackowiak, R.S., 1991. A direct demonstration of functional specialization in human visual cortex. J. Neurosci. 11 (3), 641–649.